University of South-Eastern Norway
Faculty of Health and Social Sciences
–
Master's Thesis
Master of optometry and visual science
Spring 2023

Kristian Brekstad

Gonioscopic findings in young adults assessed by means of 360-degree goniophotography

A pilot study using the Nidek GS-1 Gonioscope.

Distribusjon av gonioskopiske funn på goniofotografier av unge voksne.

En pilotstudie utført med Nidek GS-1 Gonioscop

University of South-Eastern Norway
Faculty of Health and Social Sciences
Department of Optometry, Radiography and Lighting Design
PO Box 235
NO-3603 Kongsberg, Norway

http://www.usn.no

Summary

Purpose: The primary objective was to investigate the visibility of angle structures and gonioscopic findings in four quadrants in young eyes by means of 360-degree goniophotography acquired by the Nidek GS-1 Gonioscope (GS-1).

Background: The anterior chambre angle is where the majority of the aqueous, produced in the ciliary body, is drained through the trabecular meshwork. Despite being dependent on the skill of the examiner, indirect gonioscopy remains the reference standard for a qualitative examination of the anterior chambre angle. This dependence on the skill of the examiner may be a limiting factor when performing qualitative studies on the ACA. The knowledge of normal variations such as trabecular pigmentations, iris processes, blood vessels and goniosynechiae is limited. Launched in September 2018, the Nidek GS-1 Gonioscope (Nidek, Japan) is a dedicated camera for goniophotography. It provides a 360-degree photograph of the anterior chambre angle.

Methods: The study had a cross-sectional design. Subjects was recruited from the students at the University of South-east Norway, campus Krona. Goniophotography was performed using the Nidek GS-1 automated gonioscope. Image quality and normal variations was registered and graded by an optometrist trained in the use of the gonio camera. Descriptive values included was central values (mean, mode) and spread of values (standard deviations, quantiles). Inferential statistics included correlation, and comparison between groups (Two-sample Wilcoxon, Friedman rank-sum).

Results: In total, 51 eyes of 27 subjects, 10 males and 17 females, were photographed. Mean age was 25,4 years. The percentage for best grade of image quality for the superior, inferior, temporal and nasal quadrant was 70%, 90%, 84% and 82% respectively, the difference was significant. There was no significant bilateral asymmetry. The most common grade for angle opening was 4 with the inferior quadrant having a significantly lower graded angle opening. Trabecular meshwork pigmentation was found in 96% of the eyes with the inferior quadrant being significantly the most pigmented. Iris processes was found in 86% of eyes. Here the superior quadrant, with significance, had the lowest grading. Blood vessels was found in 23% of the ACA while no goniosynechiae was observed.

Conclusion: The GS-1 provided images where the ACA structures was at least partially or fully focused for identification in 99% of the eyes. This makes it a highly suitable instrument for both scientific studies and for clinical use. The ciliary body was visible in 94% of the eyes, the inferior quadrant had the narrowest angle opening. Found in 96% of the eyes, trabecular meshwork pigmentation was the most common normal variation with the inferior quadrant being the most pigmented. Iris processes was found in 86% of the eyes with the superior quadrant having the lowest amount. BVs was found in 23% of the eyes without any quadrant differing and no goniosynechiae was found. There was no significant difference between the eyes.

Keywords: Anterior chambre angle, Nidek GS-1, trabecular pigmentation, gonioscopy

Contents

Foreword

I would give a big thank to Per Olof Lundmark, my excellent supervisor! Your suggestions and numerous corrections are a big part of this thesis. A special thank goes to Irene Langeggen along with a little nod to Hans Thorvald Haugo for assistance during the second round of recruitment. To my fellow classmates: congratulations on your degrees and a large thanks. Keeping the spirits up during long days and a world wide pandemic was a challenge but we slayed that beast! For their help with logistics during both school days and crashed cars, May-Linn and Haakon have my deepest gratitude! My colleagues in Krogh Optik Tønsberg deserves a round of applause, for providing me with a workplace second to none and giving med energy for the studies. Thanks all those that volunteered their eyes: without you this thesis would only be theoretical.

And lastly to my dear Kristin. Thank you for keeping me fed and upright during these five years of study. From now on you will no longer have to look into a study room containing more glasses and plates than the kitchen. I love you!

Siljan, 27.04.23

Kristian Brekstad

1. Background

1.1.Anatomy and physiology of the anterior chamber

The corneal posterior surface marks the anterior boundary of the anterior chamber (AC) while the pupillary margin and the anterior surface of the iris constitute the posterior one. They join together with the peripheral boundary, defined by the anterior surface of the ciliary body, in the anterior chamber angle (ACA). This is sometimes referred to as the drainage angle. The ACA is where the majority of the aqueous (AH), produced in the ciliary body, is drained through the trabecular meshwork, into the canal of Schlemm and from there into the venous system of the episclera. Obstruction of the aqueous outflow can cause an increase in intraocular pressure (IOP), causing damage to ocular structures. Such obstructions can stem from trauma, misplacement of the iris and/or any innate or acquired abnormalities (Kanski, 2007; Wolff, Bron, Tripathi, & Tripathi, 1997). Listed in an anterior-posterior order, the ACA consist of the Schwalbes line (SL), the trabecular meshwork (TM), the scleral spur (SS), the ciliary body (CB) and the iris root (IR) (fig. 1-1).

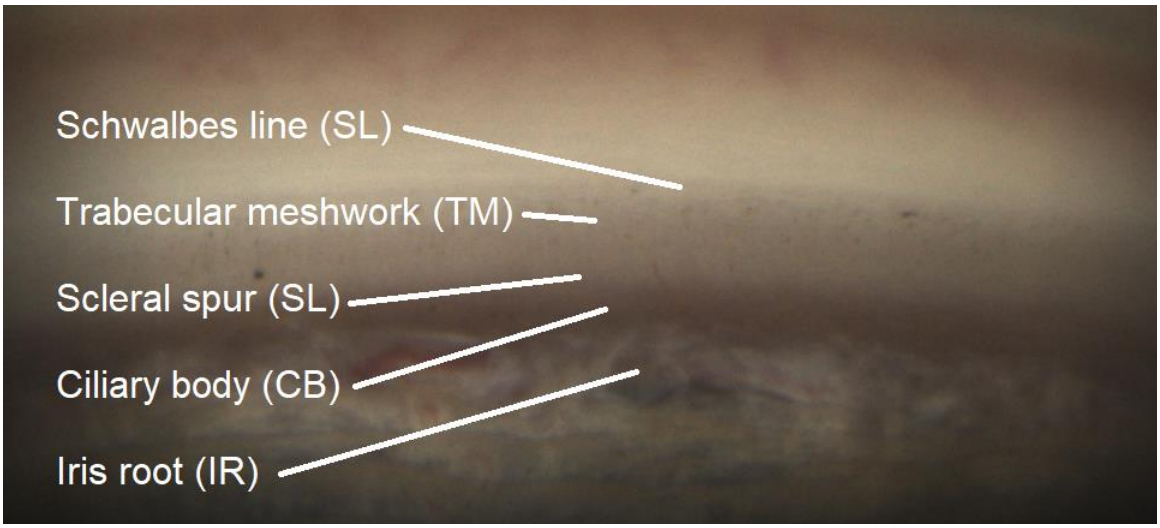

Figure 1-1: view of the ACA. Captured with the Nidek GS-1 automatic gonioscope.

1.1. Blood supply and innervation of the ACA.

As with the rest of the eye, the ACA receives its blood from the ophthalmic branch of the carotis interna artery. The SL, TM and the SS being composed of mainly collagen fibres and water are relatively avascular and have low metabolic activity. They are supplied by the anterior ciliary arteries splitting off from the larger arteries in the four extraocular recti muscles. The posterior ciliary arteries supplies the CB and iris (Wolff et al., 1997). Due to their scleral insertion via the rectus muscles, the anterior ciliary vessels are prone to disruption during surgery for both strabismus and retinal detachments. This disruption increases the risk of anterior segment ischemia resulting in loss of the blood-aqueous barrier (Pineles et al., 2018). The anterior and posterior ciliary arteries form the arterial circles within the CB and iris respectively. Though thin, there are anastomoses between the branches of the ciliary arteries (Ansari & Nadeem, 2016). The blood from the iris and the CB are exits via the posterior ciliary veins. The veins from the ACA are integral for the circulation of both blood and as described below, the AH from the Schlemms canal (Ansari & Nadeem, 2016; Wolff et al., 1997).

The sensory innervation of the ACA is provided by the nasolacrimal branch of the ophthalmic nerve, itself a branch of the trigeminal nerve (Wolff et al., 1997). The fibres are found inserted into the SS, within the structure of the TM and on the endothelial cells of the Schlemms canal peripheral to it. They are believed to be of both afferent and efferent type. Through different roles and mechanisms, these fibres helps to regulate the AH outflow. Fibres of the nasolacrimal nerve also runs through the ciliary ganglion, entering

the eye alongside sympathetic fibres to the dilatator muscle in the iris, in one of the short ciliary nerves. (Wolff et al., 1997). The ACA is affected by sympathetic and parasympathetic innervated muscles, all innervated by occulomotorius fibres via the ciliary ganglion. The CB, parasympathetically innervated, causes structurally changes in the TM as described later (Boote et al., 2020; Wolff et al., 1997).

1.2. Schwalbes line

SL is as previously stated the anterior border of the ACA where the corneal endothelium transitions over to the TM. It is also where the Descemet´s membrane terminates (Wolff et al., 1997). When examining the ACA with the gonioscope the SL appears as a thin, pale line anterior to the TM. A recommended method for locating it is setting a narrow light slit and observing where the light on the anterior and the posterior cornea intersect (W. L. M. Alward, 2008). Histologically it consists of circularly arranged collagen fibres. Viewed in a scanning electron microscope it has a smooth appearance, providing the alternate name of limbal Smooth Zone. Its width varying between 50-150µm, the average being 79±22 µm with greater numbers supero-temporal (Breazzano, Fikhman, Abraham, & Barker-Griffith, 2013). There is possibly a correlation between the width of the SL and the distance from the extraocular muscles to the cornea (Breazzano et al., 2013; Spencer, Alvarado, & Hayes, 1968).

There has been found stem-cells at the posterior border of the SL. Though these cells are capable of undergoing differentiation into corneal endothel-cells, it is uncertain whether new cells are able to perform the normal functions (Sie et al., 2020). This points to that the SL plays a role in a repair process for both the TM and to a limited degree the corneal endothelium (McGowan, Edelhauser, Pfister, & Whikehart, 2007; Whikehart, Parikh, Vaughn, Mishler, & Edelhauser, 2005).

1.3. Trabecular meshwork

Covering the canal of Schlemm as a sieve, the structure of the TM is organised in a sponge-like structure. In a gonioscope it has a pale grey colour if unpigmented, getting darker with age and increased pigmentation. Approximately 750µm wide and ~150µm deep (Wolff et al., 1997). The theory of the TMs role in drainage of AH was proposed by Schwalbe I 1870 and proven by Seidel and Ascher in 1921 and 1942 respectively (Ascher, 1942; Seidel, 1921) It is responsible for about 70% of the aqueous outflow, the remaining 30% takes the uveoscleral rout (Srinivas, Guidoboni, Burli, Harjai, & Kompella, 2021; Wolff et al., 1997). Histologically it can be divided into three parts (fig. 1-2). From inner to outermost these are the uveal meshwork (UM), the corneoscleral meshwork (CM) and the juxtacanalicular meshwork (JCT). The UM and CM consist of collagen and elastin covered in TM-cells. In the UM the fibres are organized as individual lamellae with open spaces in between while in the CM they are layered as perforated plates. The JCT is TM-cells surrounded by extracellular matrix, forming a loose connective tissue 2-5 layers of cells deep. The gaps between the fibres are larger at the AC, getting smaller nearer the Schlemms canal (Stamer & Clark, 2017). The JCT is separated from the canal of Schlemm (SC) by a layer of connective tissue. The SC is lined by a single layer of endothelial cells and. The histological appearance and surrounding tissue of the inner wall cells (ACA-side) differ from those on the outer wall. The latter are longer, smoother and flatter. Also, the outer basal laminae are thicker and more continuous. The SC is drained via the collector channels to the episcleral veins. (E. R. Tamm, 2009; Wolff et al., 1997). A common phenomenon during gonioscopy is blood reflux in the SC. It is characterized by venous blood in the SC resulting from either occluded episcleral veins, most common from the gonioscopy lens, or reduced IOP, making the SC appears as a red line in the region of the TM. It is possible that blood reflux is indicative of the venous drainage resistance and thus can have predictive value for the efficiency of trabeculoplasty in patients with primary open angle glaucoma (Gong, Al-Wesabi, Zhao, & Zhang, 2018; Grieshaber, Pienaar, Olivier, & Stegmann, 2010).

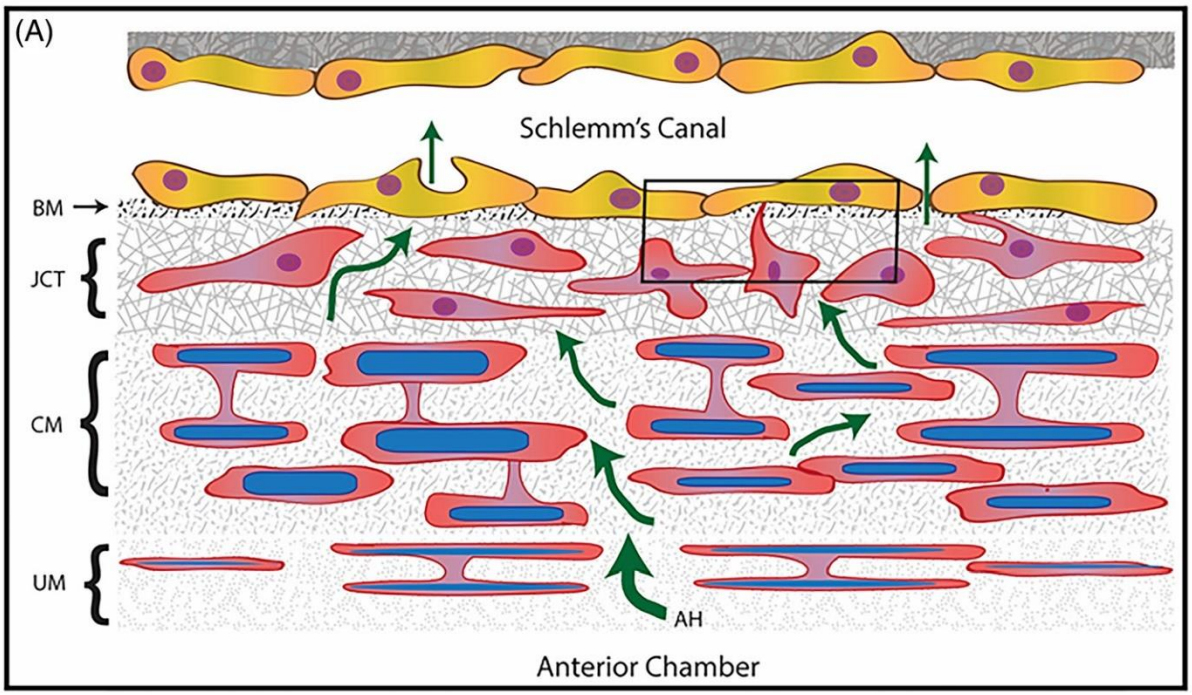

Figure 1-2: schematic presentation of the morphology of the TM and the SC. Reprinted with permission (Keller & Peters, 2022)

Studies have revealed that the TM-cells are capable of multiple functions dependent on their location. The can line the aqueous channels, remove material obstructing AH outflow via phagocytosis and produce extracellular matrix, functioning as connective tissue cells (Coulon et al., 2022). In the UM of glaucomatous eyes, the number/density of cells are lower. One of the theories regarding dysregulation of IOP in glaucoma is based on a lack of sensory feedback from the UM to the JCT, stemming from loss of cells (Costagliola et al., 2020).

1.4. The scleral Spur

The SS is the circumcorneal anterior termination of the deep scleral collagen fibres, giving it a pale appearance in gonioscopy. Narrower in persons with primary open angle glaucoma, in healthy eyes its width is about 170 µm (Boote et al., 2020). It is composed of collagen fibres, a variant of smooth muscle fibres (microfibroblasts) and elastin fibres. Posteriorly, the muscle fibres of the CB are attached while the anterior collagen fibres are interwoven with and increasingly covered by cells of the TM (Boote et al., 2020; Li, Luo, Yan, & Zhang, 2020; E. Tamm, Flügel, Stefani, & Rohen, 1992). Because of the CB fibres attached in the SS, contractions in the CB causes a posteriorly shift of the SC. This shift coupled with contractions of the microfibroblasts increases tension on the TM, opening it up and increasing aqueous outflow (Wolff et al., 1997). There is also evidence for mechanosensory nerve endings (Wolff et al., 1997). Several functions of these receptors have been theorized. One possibility is providing proprioceptive information for the CB or the SS-fibres. Another suggested function is acting as a sensor picking up changes in IOP via changes in mechanical force exerted on the SS (E. R. Tamm, 2009).

1.5. The ciliary body

The CB is a complex structure of which only the most anterior 1-1.5 mm is viewable using gonioscopy. Circular and approximately 6.5mm wide, the CBs roles are production of AH, regulation of AH drainage and accommodation. Its main components are the supraciliary layers, the ciliary body, the stroma and the epithelial layers (Fernández-Vigo et al., 2022). Comprised by smooth muscle fibres, parasympathetically innervated from the oculomotors nerve, the anterior ciliary muscle is viewable in ACAs with a wide opening. The ciliary muscle is divided into three parts differentiated by the orientation and function of the fibres. The external fibres, closes to the sclera, are oriented longitudinal. The fibres of the intermediate part are obliquely oriented, and the internal ones are circular running parallel to the limbus. It is the longitudinal fibres, visible during gonioscopy, that insert into the SS, helping to regulate the aqueous outflow (Wolff et al., 1997). The blood-aqueous barrier is composed of several structures in the CB preventing unregulated movement of substances from the plasma to the AH. The main barrier is believed to be the tight junctions of the non-pigmented epithelial cells in the ciliary processes. Disruption of the blood-aqueous barrier can in certain pathological circumstances be beneficial increasing AH proteins and white blood cells. In other cases the disruption increases the risk of complications as cataracts and synechiae (Stamper, Lieberman, & Drake, 2009).

1.6. Iris root

Also known as the ciliary zone, with a thickness of 0.5mm the iris root is the thinnest section of the iris. Histological in an anterior-posterior order it consists of the anterior border layer, stroma, anterior epithelium with the dilator muscle and the posterior pigmented epithelium. The iris root is where the iris dilator muscle is connected into the ciliary body (Garcia, Spielberg, & Finger, 2011; Wolff et al., 1997). The uveoscleral route for drainage of AH was first described in primates in 1965 (Bill, 1965). Flowing into the porous iris base and further into the ciliary body, the flowrate of AH is unaffected by IOP and constitutes roughly 30% of the total AH outflow (Yucel & Gupta, 2015). Though the uveoscleral flowrate is constant regardless of IOP, common treatments for glaucoma like prostanglandin analogs and prostamides targets the uveoscleral pathway increasing outflow and thus lowering IOP (Cheuk, Kumar, & Du, 2022).

1.7. Secretion and drainage of aqueous humor.

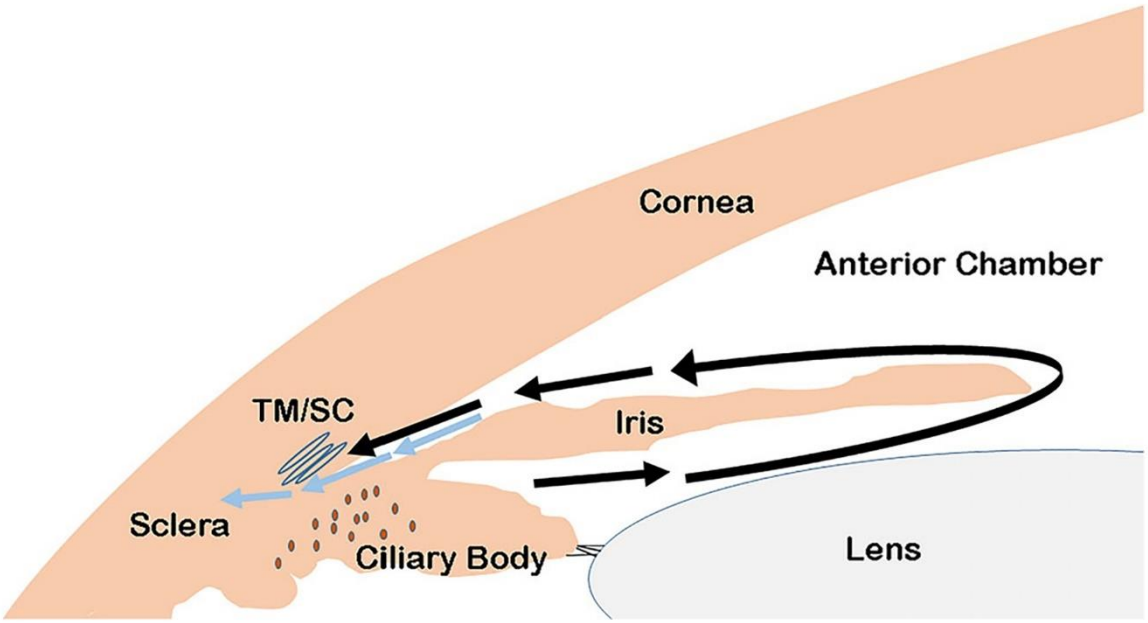

Figure 1-3 : schematic illustration of the AHs (black arrow) flow from the posterior CB, into the AC being drained through the TM. Used with permission (Keller & Peters, 2022)

The AH is secreted from the epithelium of the ciliary epithelium (fig. 1-3). Ions are actively transported over the epithelium resulting in an osmotic flow of water into the posterior chamber. Ranging from 2.2-3.1 ml/min and unaffected by IOP, production is not found to be abnormally high in any kind of glaucoma (Malihi & Sit, 2011). The AH then flows from the posterior chamber exiting into the AC through the pupil. The majority of AH-drainage from the AC, as stated above, occurs via the TM into the canal of Schlemm. The majority of the AH outflow trough the TM, occurs in the inferior quadrant, followed by the nasal (Cha, Xu, Gong, & Gong, 2016; Giusti, Pajaro, & Tanito, 2018). Then from the canal, via 25-35 irregularly spaced collector channels, into three interconnected venous plexuses and from there into the episcleral veins before continuing into the anterior ciliary vein. Often this is called the conventional outflow pathway (Johnson, McLaren, & Overby, 2017; Wolff et al., 1997). The majority of resistance to aqueous outflow occurs in the JCT and the Schlemms canal. The exact mechanisms for control of the outflow and thus regulation of the IOP is unknown. What is known is that the TM is susceptible to variations in the mechanical strain resulting from variations in IOP, altering its structure. The structural changes have been shown to cause alterations in several processes of the TM-cells and the inner walls of the canal of Schlemm (WuDunn, 2009). The TM rate of outflow is affected by the IOP and the episcleral venous pressure. Decreasing with age, the TM outflow is ~0.25µl/min/mmHg. The uveoscleral outflow is not IOP sensitive and estimated at ~1.64 µl/min (Malihi & Sit, 2011; Toris, Yablonski, Wang, & Camras, 1999).

1.8. Examining the ACA

A major challenge when examining the ACA, is overcoming the total internal reflection that happens when the light from the ACA is reflected by the tear-air interface back into the AC. Unintentionally in 1898, the first examination of the ACA in a living person was performed. Trying to see the ora serata and the CB, the Greek ophthalmologist Alexios Trantas eliminated the internal reflection by using an ophthalmoscope and indenting the sclera. The resulting displacement of the ACA made the light exit the cornea at a steep enough angle, avoiding total internal reflection. The first gonioscopic lens giving a direct view of the ACA (fig. 1-4, right) was made by Maximilian Salzmann in 1915. Being dependent on putting the patient in a supine position and needing a special slit lamp, direct gonioscopy is today only used in ACA surgery and for examining babies (W. L. Alward, 2011). Performed for the first time in 1938, in indirect gonioscopy the lens gives an indirect view into the ACA via one or several internal mirrors in the lens (fig.1-4 left) (W. L.

Alward, 2011; Friedman & He, 2008). Despite being dependent on the skill of the examiner, indirect gonioscopy remains the reference standard for a qualitative examination of the ACA. This dependence on the skill of the examiner, coupled with the need of several examinations per subject, may lead to inter-observer variations when performing epidemiological studies on the ACA. (Shaffer, 1960; Spaeth, 1971).

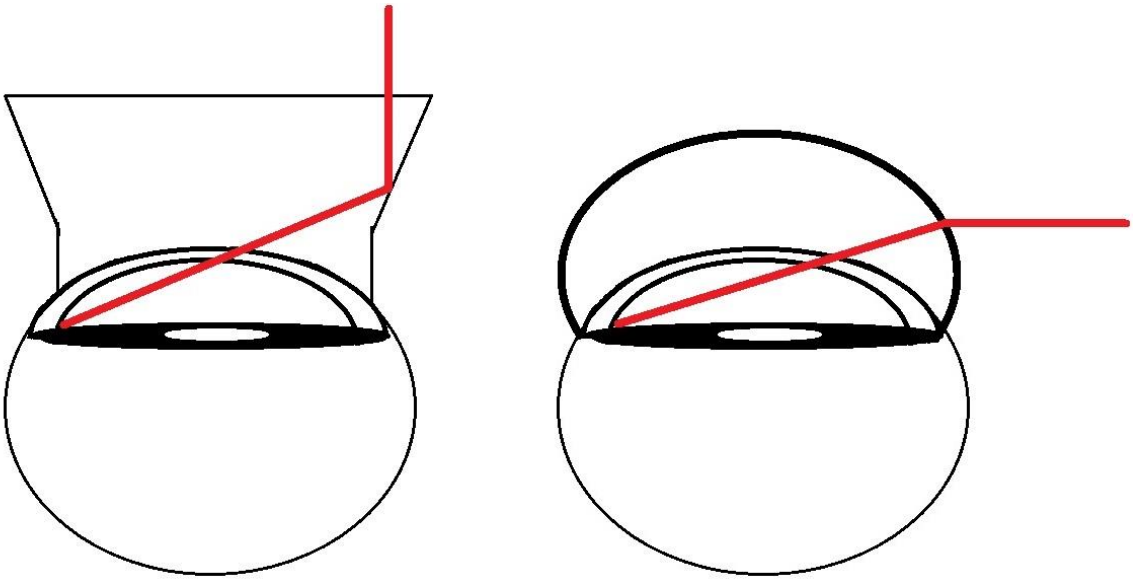

Figure 1-4: Schematic representation of the lights path (red line) in indirect (left) vs. direct gonioscopy (right)

1.9. Grading the ACA

One of the most used methods for judging the ACA width, the Van Herricks method only gives the clinician an indication on the depth of the AC compared to the corneal thickness. It provides no information about normal variations and pathology in the ACA (W. L. M. Alward, 2008; Van Herick, Shaffer, & Schwartz, 1969). For grading gonioscopy the three most common are the systems of Schaffer, Spaeth and Scheie. The former is considered to be the easiest to learn and implement. It grades the ACA opening in degrees. During gonioscopy this judgement is based on the anatomical structures visible and approximating the insertion angle of the iris in relation to the TM. If the angle opening is below 20 degrees (TM is barely visible) it is considered narrow and capable of closing (Shaffer, 1960). The Scheie grading of the ACA opening is based on the structures visible during gonioscopy. From wide open/0 (CB visible) to IV (SL not visible), angle closure is considered possible or grade III and IV (Scheie, 1957). The Spaeth system are more descriptive for the peripheral iris. It has separate grades for the iris shape, level of insertion, and its angle relative to the TM as when examined in the gonioscope. Graded from A for anterior to SL, to E for extremely deep (behind the CB), iris insertion describes the site of insertion of the iris relative to the TM. The shape of the peripheral iris can be “r” for flat or regular, “s” for steep or “q” for queer of concave. The angle is as in Shaffer, an estimation relative to the TM (Spaeth, 1971).

Spaeth also describes TM-pigmentation at the 12 o`clock angle from 0 (none) to 4+ (heavy). Included in the system is also a grade for number and types of iris processes (W. L. Alward, 2011; Spaeth, 1971). The Scheie technique are often used for grading of trabecular pigmentation, ranging from 0 (none) to IV (heavily. Most commonly this is performed by comparing the ACA of the patient to a legend/picture (Scheie, 1957)

1.10. Imaging the anterior chamber

Since they were the first to perform gonioscopy, not surprising the first illustrations of the living ACA was made by Trantas and Salzmann (W. L. Alward, 2011). This was completed in the form of detailed drawings and paintings. The first photography of the ACA was captured by Thorburn in 1927. Though the type of lens and setup is not known (W. L. Alward, 2011).

Previously limited by the skills of the practitioner, documentation of gonioscopic findings in the ACA have been accomplished by either hand drawings or slit lamp photography via a gonioscopic lens. Anterior segment OCT (AS-OCT) has in the later years provided clinicians with a low-invasive method for quantitative examinations of the ACA. AS-OCT can provide objective measurements of parameters such as AC volume, AC-depth and angle opening. A limitation of AS-OCT is the inability of performing qualitative examinations of the ACA. This means a limitation in documenting both normal and pathological findings, surgical procedures and implants (Cutolo et al., 2021). Initially developed for imaging the peripheral retina, the handheld modified EyeCam (Clarity Medical Systems, Pleasanton) takes images that cover 120-130 degrees of the ACA. It provides qualitative examinations of the ACA, have good reproducibility compared to gonioscopy and can be performed by a trained technician. However, with the patient in a supine position, poor control of the instruments light and being somewhat operator dependent, it has a tendency of overestimating the ACA opening (Perera et al., 2010; Porporato, Baskaran, Husain, & Aung, 2020)

1.11. Nidek GS-1 gonioscope

Goniophotography provides a method for documentation and assessment of the anterior chamber angle. Launched in September 2018, the Nidek GS-1 Gonioscope (GS-1) is a dedicated camera for goniophotography (fig 1-5). It is not required but topical anaesthesia is recommended. A 16-faceted multimirror prism (MMP) is mounted to the camera. Examinations are performed by placing the MMP on the cornea with the application of a coupling gel. Each of the 16 sectors (~22.5 degrees/sector) of the anterior angle is then photographed, in sequence, 5 times with varying focal plane, by a rotating internal camera. The apparatus then automatically chooses the image with the best perceived focus from each sector and presents it to the examiner. The examiner can accept the one precented or choose an image in which the focus provides more relevant information. The images can be stitched together in a single continuous picture, linear (fig. 1-6) or circular (fig. 1-7), of the complete iridocorneal angle. Examination time per eye is about 1 minute per eye (Nidek, 2018). It provides clinicians with a useful tool for documentation of anatomical structures, surgical procedures or implanted devices. It is possible for a clinician to delegate the task of taking photographs to trained assistants, secretaries or nurses (operator), freeing up time for the clinician who can examine the photograph later. The GS-1 also provides a valuable tool for the education of patients (Laroche et al., 2023).

Figure 1-3 the Nidek GS-1, screenshot from https://www.nidek-intl.com/product/ophthaloptom/diagnostic/dia_retina/gs-1.html, 19/3-23

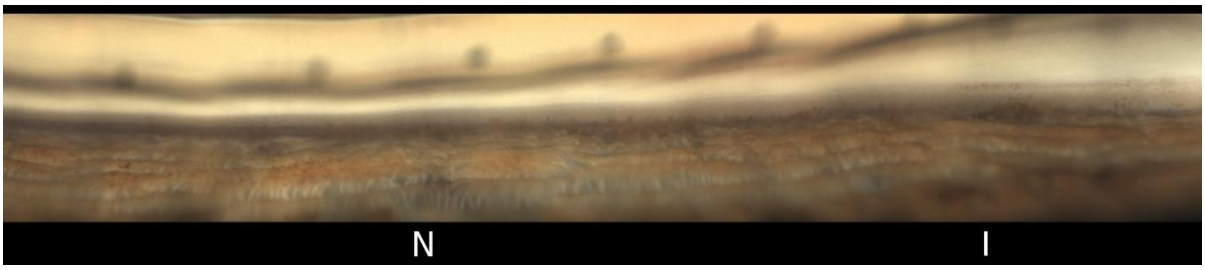

Figure 1-4: Outtake of a linear compilation.

Figure 1-5: Circular compilation of all 16 sectors forming a complete 360-degree picture of the ACA

A fairly recent tool, not many studies have been performed on the image quality (IQT) of the photographs acquired with the GS-1 (Table1-1). The first study was performed in Teixeira in 2018 using a prototype of the GS-1. Because of technical problems only 3.4% of the eyes was photographed with good focus and discernible details for 360 degrees (Teixeira et al., 2018). With technical developments the IQT have improved. In later studies Shi was successful in imaging the ACA for 91.7% of the quadrants while Barbour-Hastie captured good quality images of the entire ACA in 46% of the quadrants (Barbour-Hastie et al., 2022; Shi et al., 2019). There is also research into using software to achieve greater depth of focus in the images and for grading of pigmentation, angle opening and other normal variations (Masato Matsuo et al., 2022; M. Matsuo, Pajaro, De Giusti, & Tanito, 2019)

Study/year	[Age, standard deviation, range]	Number of eyes	Quality of images	
Teixtera 2018	63 ± 10 years Range 21-87	88 eyes of 47 subject	3.4% of eyes with all quadrants in focus.	
Shi 2019	54 ±21 years Range: 25-93	84 eyes from 50 subjects	28 (8.3%) of 336 quadrants were not gradable	Mix of healthy and glaucomatous eyes
Matsuo 2021	61.5±14.3 Range 23–83	35 eyes of 35 subjects	Mean grade 0.33	IQT graded on a 0-1 scale were 0 is best graded IQT
Barbour-Hastie 2022	69.8 ±16.6 years Range 28-85	43 eyes of 25 subjects	Good quality in 360-degrees for 46% of eyes,	

Table 1-1: Studies that graded the image quality of the GS-1 (Barbour-Hastie et al., 2022; Masato Matsuo et al., 2021; Shi et al., 2019; Teixeira et al., 2018)

The existing studies are performed on older populations and not with a large focus on the IQT and the variables affecting it. Further knowledge on what IQT the GS-1 is capable of and what influences this is needed.

1.12. Identifiable angle structures.

The ACA width/angle opening provides information on the risks of angle closure and peripheral anterior synechiaes. In the classifications of Scheies, Shaffer and Spaeth an angle is considered capable of closure if view of the TM is fully or partly obstructed in gonioscopy (Scheie, 1957; Shaffer, 1960; Spaeth, 1971). It is some evidence suggesting that the ACA-width is smaller in the superior while other suggest the inferior quadrant (He et al., 2006; Sakata et al., 2008; Shaffer, 1960). The largest ACA openings can be found in younger persons, myopes, Caucasians and pseudofakic patients (Schuster et al., 2016)

In a recent study on a Caucasian population, Jain and Zia found that 94% of the 10 491 patients had angles where the TM was mostly or fully visible. (Jain & Zia, 2021). Schuster et al, found that in the ACA of myopes, the CB was the most posterior visible structure. They found a narrower ACA opening in hypermetropes with the SS being the most posterior visible structure (Vossmerbaeumer, Schuster, & Fischer, 2013). Madu examined glaucomatous and glaucoma suspect eyes in an older population (table 1-2. They found the posterior parts of the TM being visible, meaning a narrower angle (Madu et al., 2022).

Study/year	Investigative method	Mean age	Angle opening/most posterior structure	Notes
Matsuo 2021	GS-1	61.5 ±14.3	SS	
Madu 2022	GS-1	56.4 ± 12.5	Posterior TM	
Wang 2022	Gonioscopy	4.5 years	CB	
Phu 2019	Gonioscopy		SS/CB visible in 56.1%	Healthy and glaucomatous eyes
Campbell 2015	Gonioscopy	58.9	TM visible for at least 270° in 84% of patients	

Table 1-2: Studies that stated the most posterior visible structure in gonioscopy or goniophotography (Campbell, Redmond, Agarwal, Marshall, & Evans, 2015; Madu et al., 2022; Masato Matsuo et al., 2021; Phu, Wang, Khou, Zhang, & Kalloniatis, 2019; Wang et al., 2022)

The majority of studies examining the ACA opening have been quantitative studies performed with ultrasound biomicroscopy or anterior segment OCT. Knowledge about the distribution of structures visible during gonioscopy, especially on a younger population, are limited.

1.13. Normal variations

With the examiners skill being a major limitation, epidemiological studies on gonioscopic findings are scarce. Most of the studies have either been performed in a population with the intent of detecting glaucoma or in a population with diagnosed glaucoma as a case control study. Epidemiological studies on findings such as iris processes, pigment dispersion, goniosynechiae and blood vessels in a population are few and performed on various ethnic groups. A majority of the quantitative studies have been performed with ultrasound biomicroscopy or anterior segment OCT (Doane, Rickstrew, Tuckfield, & Cauble, 2019; Gaton, Barak, Segev, Yassur, & Treister, 1998; He et al., 2006; Satoh, Takaku, Ohtsuki, & Mizuno, 1999).

1.13.1. Trabecular pigmentation

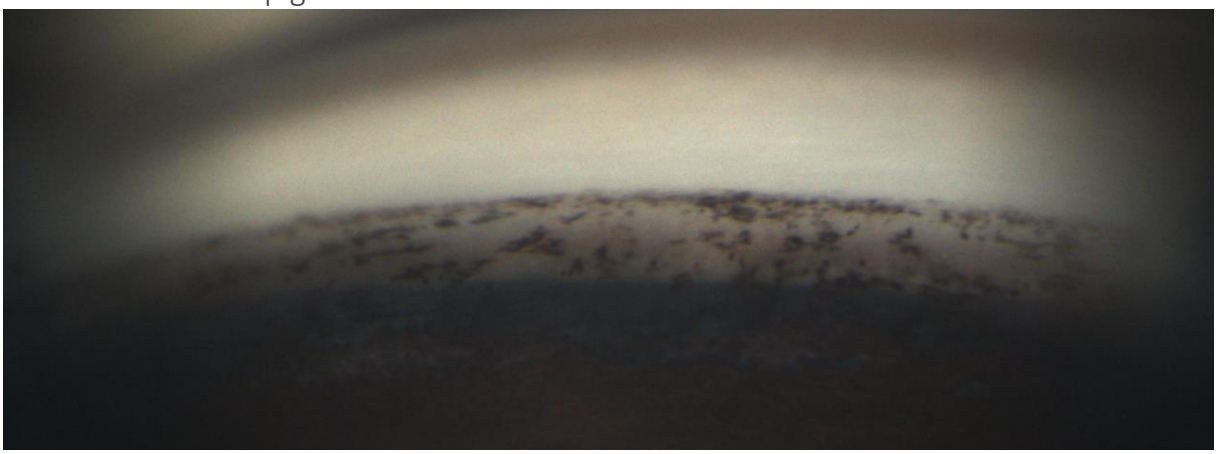

Figure 1-6: TM pigmentation in a brown eyed person.

Being a pathognomonic sign precent in 86% of patients with pigment dispersion syndrome (PDS), research into TM pigmentation (fig. 1-8) as a normal variation outside of PDS is limited (Pang, Labisi, & Wang, 2023). TM pigmentation consist of pigment particles released from the iris pigment epithelium, often from mechanical interaction with the lens or zonula threads. Following the flow of AH into the anterior chamber, the pigment particles get caught in the UM of the TM (Kanski, 2007). There they are eventually phagocytosed by the TM-cells. Over time the build-up of pigment causes changes in the gonioscopic appearance of the TM, both in the form of visible pigment particles but also the overall colour (E. R. Tamm, 2009). How this build up over time affects the physiology of the TM is currently uncertain (Gasiorowski & Russell, 2009).

Wang et. al. during preoperative gonioscopy performed on children with cataract, found TM pigmentation in 64.1% with a significant increase postoperative (table 1-3) (Wang et al., 2022). The inferior quadrant is previously found to be the most pigmented. This is not only because of gravity but is also due to the larger aqueous outflow in this quadrant (Cha et al., 2016; Masato Matsuo et al., 2021; Masato Matsuo, Pajaro, De Giusti, & Tanito, 2020).

Study/year	Population	Method	Percentage with TM pigmentation	Notes
Wang	Children with cataracts	Gonioscopy	64.1%	
Matsuo 2020	Open angle glaucoma patients	GS-1		No prevalence recorded. Inferior quadrant most pigmented.
Matsuo 2021		GS1 and gonioscope		No prevalence recorded. Inferior quadrant most pigmented.

Table 1-3: studies on distribution and prevalence of TM pigmentation (Matsuo et al., 2021; Masato Matsuo, Simone Pajaro, Andrea De Giusti, & Masaki Tanito, 2019; Wang et al., 2022)

Both the prevalence and distribution of TM pigmentation in young, healthy adults are an area where current knowledge is limited.

1.13.2. Iris processes

Consisting of uveal extensions from the anterior surface of the iris, iris processes (IP) are not a rare finding in healthy eyes. They have the appearance of small branches, either light brown in colour or in the iris colour (figure 1-9). IPs most often insert up to the scleral spur but can reach as far anteriorly as the Schwalbes line. Unlike the peripheral anterior synechiae (PAS), Ip does not interfere with movement of the iris or aqueous outflow. A PAS often is broader, have a saw-tooth like form and obstructs the view of the ACA The most precise way of differentiating IP from PAS is by indentation gonioscopy. In indentation gonioscopy pressure is applied to the cornea with the goniolens, driving the iris posterior. If there is a PAS, it will prevent posterior movement of the iris (W. L. M. Alward, 2008). Though the consensus on IP is that they do not interfere with aqueous outflow, a positive correlation with glaucoma suggest that they are ndicative of abnormal morphology in the ACA (Kimura & Levene, 1975; Wang et al., 2022)

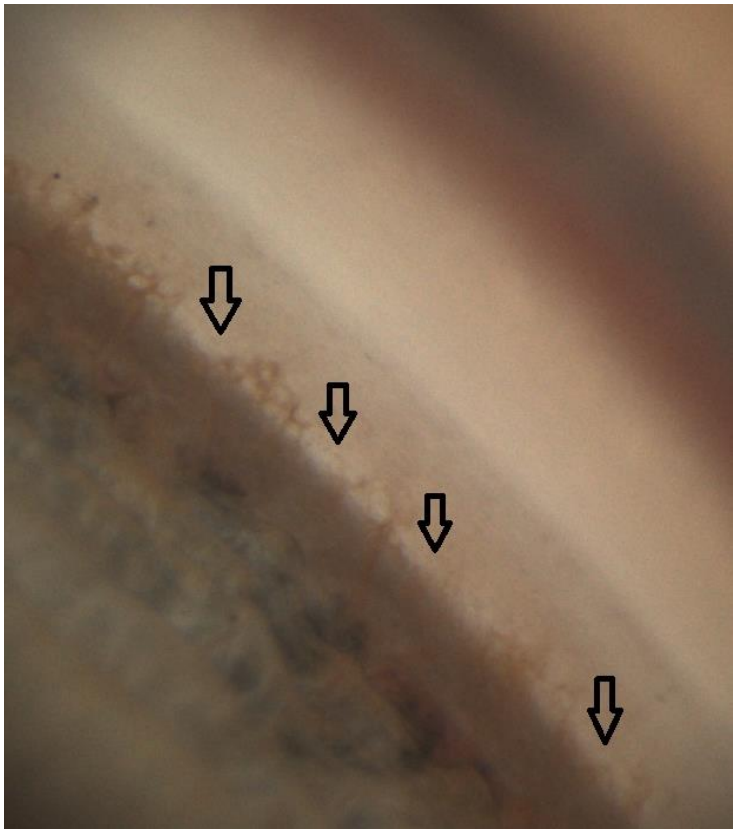

Figure 1-7: iris processes inserting into the TM. SL can be seen as the pale line indicated by the arrows.

Lichter examined 340 normal eyes, using gonioscopy, found Ips in 193 (56.7%) of them. Comparing the eyes per subject, he found a bilateral symmetry in both distribution and density in both IP and other findings (Lichter, 1969). Kimura and Levene using gonioscopy compared normal to glaucomatous eyes, grading the IP on a 0-3 scale where 0 was none. Not stating the prevalence, they discovered a higher grading (2.42 vs.1.82) in glaucomatous vs. normal and a more anterior point of insertion. Also they found a higher grading in myopes and people of African ethnicity (Kimura & Levene, 1975).Wang et. al. was examining 64 eyes with cataract in 41 children. Using gonioscopy, they found IP in 78.1% of the preoperative eyes (Wang et al., 2022). During postoperative examination they discovered a significant increase in prevalence, postoperative IPs was found in all eyes, and density of the IP. This increase was not present in the healthy eye in patients with monocular cataracts. They theorized that in addition to being congenital, IP can form resulting from an inflammatory response in the AC (Wang et al., 2022).

The prevalence and distribution of IPs in healthy, young adults are a subject in need of further research.

1.13.3. Blood vessels

As previously mentioned, the veins of the limbal scleral are responsible for about 70% of the AH outflow, but not visible in the ACA. Non-pathological blood vessels of the ACA visible in gonioscopy, are protruding from the anterior parts of the CB. They are branches of the major arterial circle, itself a meeting point of both the anterior and the posterior ciliary arteries (Wolff et al., 1997). Being both normal and pathological in nature, the blood vessels (BV) placement relative to the SS is a common way of differentiating between the two (figure 1-10). Normal vessels can be found close to but never anterior of the SS (Raluca et al., 2015).

Figure 1-8: Blood vessels in the ACA

Examining by gonioscope 269 healthy eyes, Henkind found 198 (74%) to be without visible blood vessels in the AC (table1-4). Excluding radial iris vessels, ACA vessels was found in only 36 (13%) eyes (Henkind, 1964). Chatterjee discovered vessels located in the ciliary body in 65% of healthy eyes. Satoh et. al. was examining fluorescein leakage from ACA-vessels and found them in 28% of healthy eyes. ACA vessels are found more frequently in blue eyes as they are more visible in the less pigmented CB (Chatterjee, 1960; Satoh, Takaku, Ootsuki, & Mizuno, 1992).

Study/year	Method	Percentage with vessels	Notes
Chatterjee 1960	Gonioscopy	72%	100 healthy eyes
Henkind 1964	Goniocopy	26%	269 healthy eyes
Shihab 1985		21%	
Satoh 1992	Fluorography w. trabeculens	29%	

Table 1-4: Studies on prevalence of BVs in the ACA. (Chatterjee, 1960; Henkind, 1964; Satoh et al., 1992; Shihab & Lee, 1985)

There is a lack of well documented prevalence studies for BVs in the ACA. Further knowledge regarding the prevalence, bilateral symmetry and distribution is needed.

1.13.4. Goniosynechiae

First described by Saltzmann in 1914, goniosynechiae or peripheral anterior synechia (PAS), are a condition in which the iris adheres to the CB, TM or the corneal backside (Kanski, 2007; Tandon & Alward, 2015). Pathognomonic of angle closure, it can develop following various inflammatory conditions, post-traumatic or after ocular surgeries. It is more common in narrow angles (He et al., 2006; J. Y. Lee, Kim, & Jung, 2006; T. E. Lee, Yoo, & Kim, 2021). Several studies have found PAS to be more frequent in the superior quadrant of the eye. Explanation for this varies from hydrostatic pressure of the AH in the posterior chamber, physiological decentration of the lens to peripheral flattening and posterior

movement of the superior cornea from eyelid pressure. (J. Y. Lee et al., 2006). Not always easily differentiated from IPs, PAS are often thicker and less transparent while IPs are featherier and more delicate in appearance. IPs rarely obscures the SS. As previously mentioned, PAS will prevent posterior movement of the iris during indentation of the cornea during gonioscopy (W. L. M. Alward, 2008). There has been some uncertainty whether PAS can develop in eyes without history of trauma, pathology or surgery. Foster et al. found PAS in 4% of an east-Asian population, the odds increased with the narrower angles (Foster et al., 2004). In 1405 eyes, He et al. found PAS in 2.6%, again with increased odds in angles where the posterior TM was not visible (He et al., 2006)

Despite being a pathological sign, PAS can occur in otherwise healthy eyes. Further knowledge on prevalence and distribution is needed for a deeper understanding of the formation of them.

Because there are few epidemiological studies on normal variations found in the ACA, especially on a young and healthy population, the purpose of this study was investigating the GS-1s applicability as a method in larger studies. This thesis is partly based on the project protocol, presented as the final exam in MMET4001-1, Forskningsmetoder og etikk (Brekstad, 2019, unpublished) at University of South-east Norway (USN).

2. Issue/research questions and significance

The primary objective was to investigate the visibility of angle structures and gonioscopic findings in four quadrants in young eyes by means of 360-degree goniophotography acquired by the Nidek GS-1 Gonioscope (GS-1).

The primary objective was based on the following research questions:
In healthy adults between 18-35 years who undergo 360-degree goniophotography with the Nidek GS-1 instrument:

1. What is the distribution of images quality in four quadrants assessed on goniophotographs from the right and left eye?
2. What is the distribution of visible angle structures in four quadrants identified on goniophotographs from the right and left eye?
3. What is the distribution of pigmentation, iris processes, blood vessels and goniosyncechia, in four quadrants identified on goniophotographs from the right and left eye?

The study was expected to identifying challenges in performing a prevalence study and to provide knowledge about the variability of findings in the four quadrants in young eyes obtained with goniophotography. Results were expected to give an indication of the applicability of the GS-1 as a method for documenting the ACA and normal variations in it for prevalence studies.

3. Methods

3.1.Design

The study had a cross-sectional design.

3.2.Participants

Approval for from the Regional Ethics Committee (Regional Etisk Komite) was acquired prior to starting recruitment and the data collection. Permission for storing personal the information of the subjects was granted by the Norwegian centre for research data (NSD) All measurements were performed at the National Centre for Optics, Vision and Eye Care at University of Southeast Norway (USN), Kongsberg, Norway. Those eligible to participate were males and females, aged 18-35, recruited amongst the

students attending the University of Southeast Norway, Campus Kongsberg (USNK), in the period august 2020 to October 2022. Because of Covid-19 regulations, USNK was periodically fully or partially closed until august of 2022, hindering the recruitment process. Flyers (annex 3**)** summarising the purpose and methods of the study was both posted and handed out at USNK. The flyer was also posted to social media pages (Facebook, Canvas) for students attending USNK. Those who were interested contacted the project manager, Kristian Brekstad (KB), utilizing the contact information contained within the flyer. The project manager also gave a short presentation in front of a class of optometry students. An appointment for examination was made and written consent (annex 1) was obtained prior to starting the examination. Names was replaced with a unique randomized id-number in order to ensure anonymity of the participants. All data was registered under the ID number. The list connecting the subjects and their ID number was deleted at the completion of the project. Exclusion criteria was history of adverse reactions to topical anaesthetics, active sterile or infectious pathology of the cornea and/or images of so low quality that no anatomic structures were visible. If pathology was suspected, an appointment for further examinations was to be scheduled at the clinic of the Faculty of Health and Visual Science, USN campus Krona.

3.3.Measurements

The test procedure was explained to the subject and ethnicity and eye colour was recorded. An initial subject history was taken with the project manager asking standardized questions from a form (annex2). Previous ocular trauma and systemic pathology possibly affecting the configuration of the ACA was noted as 0 (no) or 1 yes). The age was defined as date of examination minus the date of birth rounded off to the nearest year and noted. Gender was registered as 0 for male and 1 for female. Subjects wearing contact lenses removed them. Refraction and keratometry was measured by autorefractor (Topcon TRK-1P, Japan). For refraction the spherical equivalent was recorded in 0.25 dioptre steps while the keratometry was noted in millimetres in 0.01 steps. The intraocular pressure (IOP) was noted in mmHg after measurement with Icare (Rodenstock Norway). After instilling both eyes with topical Oxibuprokain 0.4% (Bausch Health, Ireland Ltd.), the central corneal thickness was measured with the Reichert Ipac (Medistim, Norway) and noted in µm. Then the illumination of the room were dimmed below 50 lux, and pupil size was measured after 1 minute, using a ruler (R. Y. Lee, Lin, Chen, Barbosa, & Lin, 2016).

3.3.1. Nidek GS-1 goniophotography

Images of the ACA was obtained via goniophotography, performed with the Nidek GS-1 Gonioscope (Rodenstock AS, Norway). The subject ID was saved on the GS-1 with Person as their first name and the assigned ID-number as their last name. A disinfected multimirror prism (MMP) was attached to the GS-1 in compliance with the manual.

The subject was seated, and both the table and the chinrest for the device was adjusted so that the subject obtained a good posture (fig. 3-1). After correct posture was obtained the subject sat back. To both protect the subjects cornea and eliminating the tear-air interface, the coupling gel was applied to the concave front of the MMP.

Figure 3-1: illustrative picture showing correct positioning and posture of the subject. The person pictured is not among the subjects in the study. Photography with consent.

To ensure a consistent application, the gel-tube was squeezed with the tip tilted upwards pushing out gel containing bubbles. After removing the faulty gel, the tip of the tube was placed against the upper section of the concave front of the MMP. Then the coupling gel was applied to the sterile MMP in accordance with the user manual in sufficient quantity, covering the surface of the prism tip completely. Verifying the application of the gel was accomplished using a dimmed penlight shining upwards from the MMPs 6`oclock position. If the gel contained bubbles (fig.3-2) or the amount was insufficient, the gel was wiped off with a clean tissue and reapplied.

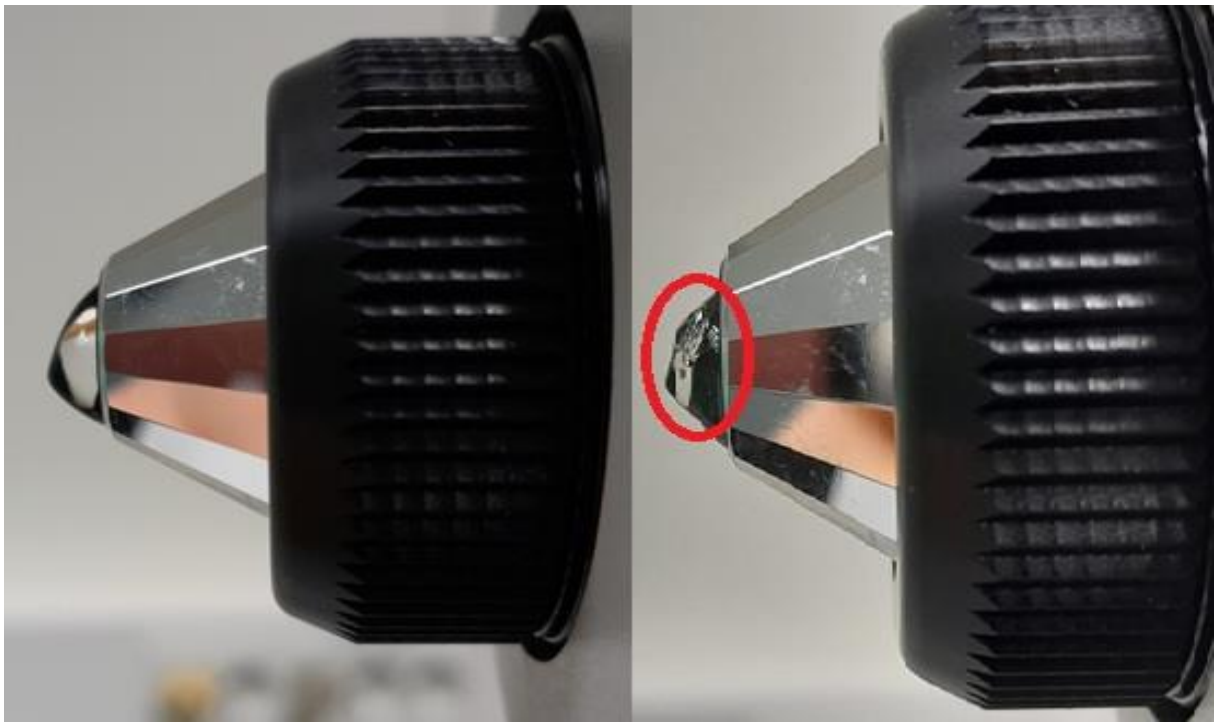

Figure 3-2: the MMP on the left have a sufficient amount of gel without bubbles. The right picture shows bubbles in the gel (red circle)

With the gel applied correctly, the subject was positioned in the headrest and instructed to fixate at the red fixation light in the GS-1 without blinking. In case of failure to maintain fixation, an external fixation light was used. The first eye to be photographed was systematically altered between right and left eye for consecutive subjects. This was done in order to avoid possible errors stemming one eye always being photographed first, known as sequential information bias.

Figure 3-3: illustrative picture showing contact between the MMP and the patient. The person pictured is not among the subjects in the study. Photography with consent.

The capture process itself was started. The subject was told to blink a couple of times before the operator (K.B), keeping the subject's eyelids lifted, slowly moved the GS-1 closer to the patient until the gel touched the cornea (Fig. 3-3). Using the joystick, the alignment was adjusted in accordance with the manual. After pressing the capture button on the joystick, once correct alignment was detected by the GS-1 the photography sequence started automatically. In each sector of the MMP, the GS-1 took 5 pictures with varying depth of focus. With each sector covering 22.5 degrees together the 16 sectors covered 360 degrees of the ACA. If the capture process exceeded the maximum time of 3 minutes and 45 seconds, the next eye was then photographed, and a new attempt was made afterwards. The GS-1 then saved the pictures on the internal hard drive. The subject sat back with eyes closed while the remaining gel was removed. Gel was reapplied and capture process for the fellow eye was started.

3.4.Analyses/variables

After completing the capture process the GS-1 then automatically selected the image with the best perceived focus from each of the 16 sectors of the MMP. After completing the selection, the selected 16 images were automatically compiled into two separate photographs of the ACA. One circular 360-degree and one linear, measuring 3638x3638 and 874x966 pixels respectively (Fig. 6 and 7). An overlay annotating the quadrants was automatically attached on each photograph by the GS-1. These photos in JPG format were then exported to an external computer, saved with only the subject ID, and right/left eye designation available.

Using the linear image working from left to right, the observer (K.B) worked at 100% zoom on a colour calibrated monitor, increasing magnification when examining uncertain findings. The border between the quadrants (inferior, superior, nasal and temporal) was set at halfway between each of the letters annotating the quadrant in the image (Fig 3-4). With the letters annotating the quadrants automatically placed in the centre of the quadrants, the border between them thus was set at the 1030, 0130, 0430 and 0730 o`clock positions. Image quality, the anatomical structures visible, trabecular pigmentation, iris

processes, blood vessels and goniosynechiae was graded according to the criteria described below. Each of the quadrants was graded separately.

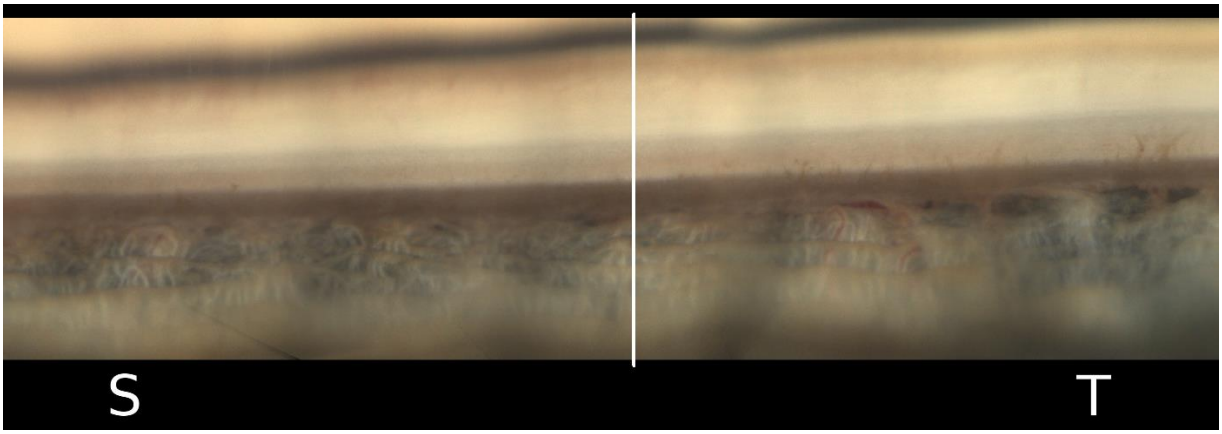

Figure 3-4: outtake from linear compilation. The white line marks the border set between the superior and temporal quadrant.

3.4.1. Grading

The grading of image quality (IQT) was decided by the focus and the illumination of the anatomical structures and normal variations, visible in the goniophotograph. It was graded in accordance with the criteria in table 1. The focus was deemed as sufficient if the anatomical structures was easily differentiated or normal variations was distinguishable. Quadrants with a grade of 0 was excluded from further analysis as to not affect the descriptive statistics.

Grade 1	Grade 2	Grade 3	Grade 0
Structures are in focus and sufficiently illuminated in the whole quadrant	Structures are in focus and sufficiently illuminated in more than half of the quadrant	Structures are in focus and sufficiently illuminated in less than half of the quadrant	Structures for assessment are not visible.

Table 3-1: grading of image quality based on Lee et al (B. Lee, Szirth, Fechtner, & Khouri, 2017)

The angle opening, were graded after the most posterior structure visible. In grade 4 it was the CB, grade 3 the SS, in grade 2 the TM and in grade 1 only the SL was visible (fig. 3-5). In ambiguous quadrants, the highest grading in a fourth or more of the quadrant was noted.

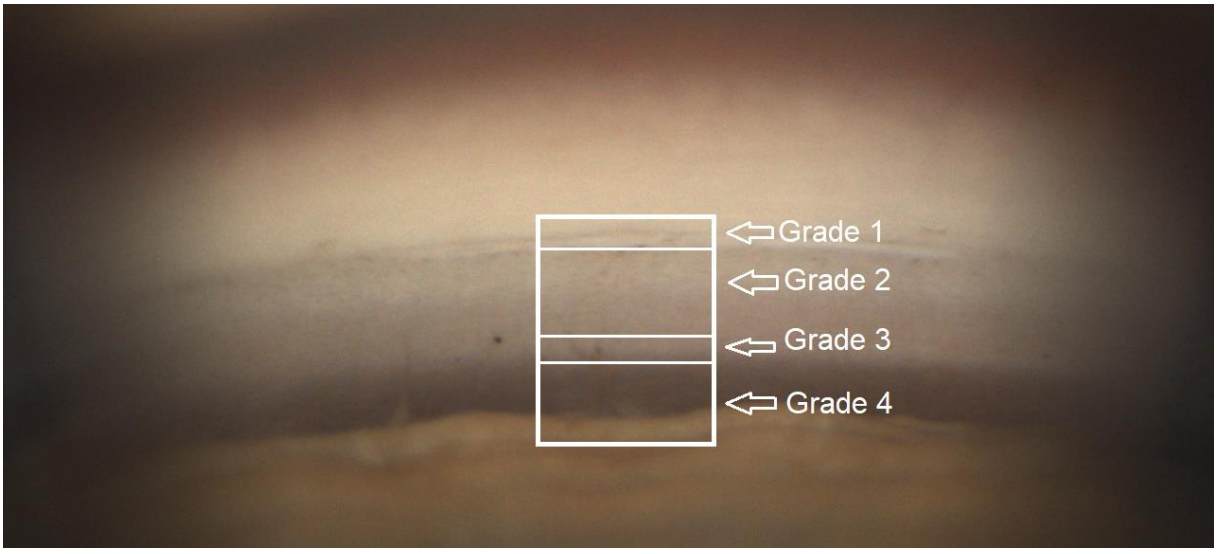

Figure 3-5: criteria for grading of angle opening.

For grading of pigmentation in the TM, the Scheies pigmentation grading was utilized (Scheie, 1957). The most pigmented section of the TM per quadrant was compared to the scale in figure 3-6. TM pigmentation per quadrant was graded from 0 (none) to 4 (the most).

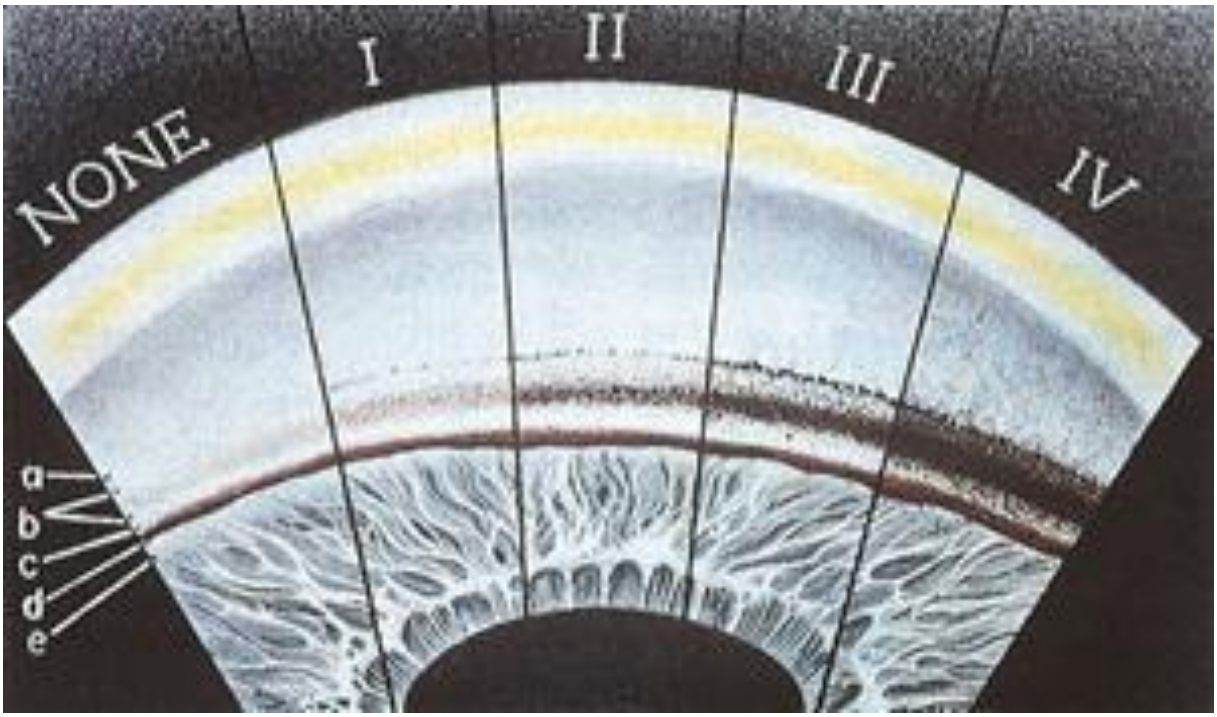

Figure 3-6: Scheies pigmentation grading. From Arch Ophthalmol. 1957;58:510–512. Copyright © 1957, American Medical Association. All Rights Reserved. Copied from https://www.aao.org/disease-review/gonioscopic-grading-systems

Iris processes was defined as small branches coloured either light brown or in the iris colour, extruding from the iris root, inserting as far anterior as the SL. Blood vessels was noted if they were located anterior to the iris root. If the iris was attached to the TM or further anterior, it was termed a goniosynechiae. These three was graded in accordance with table 3-2.

Normal variation	Grade 0	Grade 1	Grade 2	Grade 3
Iris processes	No	Precent	precent in two fourths of a quadrant.	Precent in three or all fourths of a quadrant.
Blood vessels				
Goniosynechia				

Table 3-2 grading criteria for IPs, BVs and goniosynechia

Equivocal results were graded together with a senior optometrist PL. The results from the grading were registered in data registration form (Annex 2). All the results were organised in a database (Excel, Microsoft Office) and transferred to a statistical program (R commander, The R foundation for statistical computing) for statistical analyses. Descriptive values included was central values (mean, mode) and spread of values (quantiles). Because of the low number of subjects, non-parametric testing was performed. Intereye asymmetry was analysed per quadrant using two sample Wilcoxon test. To detect any differences between the quadrants, Friedman rank-sum test was performed. Statistical significance was set to $p<0.05$ (two-sided).

3.5. Ethics

Participation was voluntary and subjects could withdraw from the study at any time without further explanation and with no consequences. All participants were given information about the study with opportunities to ask questions and to receive answer before signing the consent forms. To protect the participants anonymity, each participant was given a unique and random id-number, that did not contain any information that could be connected to the identity of the participants. The id-number was used on all data registration forms and in all datasets. The list of names with id-numbers are and will be stored safely, and distant from the data registration form and datasets. The list will be stored for five years after the project's completion and then deleted. No earlier than June 2027 and the latest date of deletion is June of 2028. This is in accordance with rules set by the Regional Committees for Medical and Health Research Ethics (REC). If there should be any indication for further examination, the participant will be referred to the clinic of The National Centre for Optics, Vision and Eye care. Ethical approval was obtained from REC and the study was registered at the Norwegian Centre for Research Data (NSD).

The use of Oxibuprokain (0,4%, Bausch Health) for local anaesthesia is a standard diagnostic drug in optometric practise. Commonly, a patient experiences a slight burning sensation when the drops are instilled, this passes quickly. Rare side effects are anaphylactic shock, dizziness, drop in blood pressure and reduces vision (felleskatalogen.no, 2023)

All procedures were non-invasive and did not cause pain or severe discomfort. Total time allocated per examination was 45 minutes. This gave plenty of time for the patient to ask questions and a short break if needed. It also gave the operator time to answer these and explain the procedures. The Nidek GS-1 goniocamera is a new device and no studies regarding the comfort of the patient have been performed. The manufacturer claims that topical anaesthesia is not required but are recommended for some patients. In this study topical anaesthesia was used on all subjects. Some discomfort for the subjects could arise during the examination due to the proximity of the MM prism tip. Without anaesthesia the gel on the eye may cause slight discomfort. The prism tip of the device is brightly but constantly illuminated for the duration of the examination, ~1 min/eye. This could cause some discomfort for those sensitive to light. All subjects prior to photography were instructed to notify the examiner if discomfort, dizziness or symptoms of fainting should arise.

4. Results

4.1.Demographics

A total of 33 persons contacted the project manager. 27 of these, scheduled an examination. 2 of the subjects did not complete the examination because of discomfort and feeling unwell during the goniophotography. In total 51 eyes of 26 persons were photographed and graded Se table 4-1 for demographics. Out of 204 quadrants photographed, 2 (1%) had an image quality not allowing the structures to be graded. The gender distribution was 17(63%) females and 10 (37%) males.

N= 27, 51 eyes		**Right eye (RE)** n=26 eyes	**Left eye (LE)** n=25 eyes
Age, years [mean, ±standard deviation(SD)]	25.4 (±0.7) Range 19-32 yrs.		
Female [n(%)] Male [n(%)]	17 (63%) 7 (37%)		
Refraction. DS [mean.±SD], range +-max DS		-0.3 ±2.3, range +4.50- -7.500	-0.4 ±2.6, range +4.00 - -10.0
CCT, µm [mean,±SD], range min-max		555.3 ±31, range 500-610µm	554.7 ±29.2, range 501-628µm
IOP, mmHg[mean,±SD,], range min-max mmHg		15.5 ±3.8, range 11-28mmHg	15.9 ±3.7, range 10-25mmHg
Keratometry, mm [mean flattest K,±SD], Range min-max mm		7.92 ±0.28, range 7.47-8.69mm	7.9 ±0.29, range 7.46-8.62m
Iris colour, [N(%)]		Blue 19 (73%) Brown 5 (19%) Green 2 (8%)	Blue 18 (72%) Brown 5 (20%) Green 2 (8%)
Quadrants photographed/not gradable		104/0	100/2

Table 4-1 demographics of the subjects, number of subjects=27, number of eyes=51. DS= dioptre sphere, CCT= central corneal thickness, µm= micrometer. IOP= intraocular pressure, mmHg= millimetres of mercury, mm= milimetre

4.2.Image quality

Table 8 precents the numerical distribution of grades per quadrant sorted per eye. Grades are sorted in a descending order with grade 1 being the best image quality. The median and inter quartile range (IQR) per quadrant is presented below each quadrant. Significant results are marked by *.

There was not any significantly difference between the IQT of the eyes. The superior quadrants had a significantly lower percentage (70%) images with top grade than the inferior (90%), nasal (84%) and temporal (82%) quadrants. There was no significant difference between the left and the right eye. In total 2 of 204 quadrants (1%) was not gradable and was excluded from further analysis.

			Count of grade, per quadrant (percentage of N)	
Quadrant	**Grade**	**Criteria for grade**	**RE (n=26)**	**LE (n=25)**
Inferior	1	Structures are in focus and sufficiently illuminated in the whole quadrant	24 (92.3%)	22 (88%)
	2	Structures are in focus and sufficiently illuminated in more than half of the quadrant	1 (3.9%)	2 (8%)
	3	Structures are in focus and sufficiently illuminated in less than half of the quadrant	1 (3.9%)	1 (4%)
	0	Structures for assessment are not visible.	0	0
Median/IQR			1/0	1/0
Temporal	1		23 (88.5%)	19 (76%)
	2		3 (11.5%)	5 (20%)
	3		0	1 (4%)
	0		0	0
Median/IQR			1/0	1/0
Superior*	1		19 (73.1)	17 (68%)
	2		7 (26.9)	7 (28%)
	3		0	1 (4%)
	0		0	0
Median/IQR			1/0.75	1/1
Nasal	1		23 (88.5%)	20 (80%)
	2		2 (7.7%)	3 (12%)
	3		1 (3.9%)	0
	0		0	2 (8%)
Median/IQR			1/0	1/0

Table 4-2: numerical distribution of grades per quadrant sorted per eye. The median and interquartile range (IQR) per quadrant is listed below the relevant quadrants. *p=0,02

4.3.Identifiable angle structures.

The most numerous, 94% of quadrants was graded opening of 4, no quadrant was being graded lower than 3 (6%). With 86% of the eyes having the grade 4, the inferior quadrant had significantly lower rate of grade 4 angle opening than the nasal, superior or temporal quadrants. They had 94%, 98% and 98% respectively (p=0.02). There was no significant asymmetry between the eyes.

Numerical distribution of gradings for identifiable angle structures is presented in table 4-3**.** Grades are sorted in a descending order. The median and inter quartile range (IQR) per quadrant is noted below each quadrant. Significant results are marked by *.

			Count of grade, per quadrant (percentage of N)	
Quadrant	**Grade**	**Posterior visible Structure**	**RE**	**LE**
Inferior*	4	4: Ciliary body	21 (80.7%)	23 (92%)
	3	3: Scleral spur	5 (19.2%)	2 (8%)
	2	2: Trabecular meshwork	0	0
	1	1: Schwalbes line	0	0
	0	0: No structures visible	0	0
Median/IQR			4/0	4/0
Temporal	4		25 (96.2%)	25 (100%)
	3		1 (3.9%)	0
	2		0	0
	1-0		0	0
Median/IQR			4/0	4/0
Superior	4		25 (96.2%)	25 (100%)
	3		1 (3.9%)	0
	2-0		0	0
Median/IQR			4/0	4/0
Nasal	4		24 (92.3%)	24 (96.0%)
	3		2 (7.7%)	1 (4.0%)
	2-0		0	0
Median/IQR			4/0	4/0

Table 4-3: numerical distribution of Identifiable angle structures per quadrant sorted per eye. The Median and interquartile range (IQR) per quadrant is listed below the relevant quadrants. *p=0,02

4.4. Pigmentation

Pigmentation in the TM was observed in 49 of 51 eyes (96%). The inferior quadrant had a significant higher grading (median 1) than the temporal (0), superior (0) and nasal quadrant (0) (p-value < 0.001). There was no significant asymmetry between the eyes. When analysing the distribution of ratings, 37% of the inferior quadrants was graded 2 or more pigmented while the temporal, superior and the nasal all only had 4% above grade 1.

Numerical distribution for pigmentation of the TM is presented in table 4-4. Grades are sorted in a descending order, grade 4 is the heaviest TM pigmentation, grade 0 is no pigment. The median and inter quartile range (IQR) per quadrant is presented below each quadrant. Significant results are marked by *.

			Count of grade, per quadrant (percentage of N)	
Quadrant	**Grade**	**Criteria for grade****	**RE**	**LE**
Inferior*	4	Excessive	0	0
	3		2 (7.7%)	2 (8%)
	2	Medium	10 (38.5%)	5 (20%)
	1		12 (46.2%)	18 (72%)
	0	None	2 (7.9%)	0
Median/IQR			1/1	1/1
Temporal	4		0	0
	3		0	1 (4%)
	2		1 (3.85%)	0
	1		12 (46.2%)	8 (32%)
	0		13 (50%)	16 (64%)
Median/IQR			0.5/1	0/1
Superior	4		0	0
	3		0	0
	2		1 (3.9%)	1 (4%)
	1		6 (23.1%)	4 (16%)
	0		19 (73.1%)	20 (80%)
Median/IQR			0/0.75	0/2
Nasal	4		0	0
	3		1 (3.9%(	0
	2		0	1 (4%)
	1		7 (26.9%)	5 (16%)
	0		18 (69.2%)	19 (80%)
Median/IQR			0/1	0/0

Table 4-4: numerical distribution of trabecular meshwork pigmentation per quadrant sorted per eye. The Median and interquartile range (IQR) per quadrant is listed below the quadrants. * p-value < 0.001 **= see figure 16, page 25, for more precise criteria.

4.5.Iris processes

IP was observed in 44 of 51 (86%) eyes. The most frequent grading was 0 with 49% of the eyes graded that. The superior quadrant had a significant lower grading of IPs, 78% of eyes graded 0 or 1, than the temporal, inferior and nasal quadrant (p<0,02). There was no significant asymmetry between the eyes.

Numerical distribution of gradings for iris processes (IP) is presented in table 4-5**.** The median and inter quartile range (IQR) per quadrant is presented below each quadrant. Grades are sorted in a descending order. Significant results are marked by *.

			Count of grade, per quadrant (percentage of N)	
Quadrant	**Grade**	**Criteria**	**RE**	**LE**
Inferior	3	Precent in three or all fourths of a quadrant.	5 (19.2%)	4 (16%)
	2	precent in two fourths of a quadrant.	5 (19.2%)	4 (16%)
	1	Precent	7 (26.9%)	10 (40%)
	0	None	9 (34.6%)	7 (28%)
Median/IQR			1/2	1/2
Temporal	3		4 (15.4%)	3 (12%)
	2		2 (7.7%)	2 (8%)
	1		11 (42.%)	13 (52%)
	0		9 (34.6%)	7 (28%)
Median/IQR			1/1	1/1
Superior*	3		2 (7.7%)	3 (12%)
	2		3 (11.5%)	3 (12%)
	1		6 (23.1%)	8 (32%)
	0		15 (57.7%)	11 (44%)
Median/IQR			0/1	1/1
Nasal	3		3 (11.5%)	3 (120%)
	2		5 (19.2%)	7 (28%)
	1		8 (30.8%)	3 (12%)
	0		10 (34.6%)	12 (48%)
Median/IQR			1/2	1/2

Table 4-5: numerical distribution of IPs per quadrant sorted by eye. *P<0,02

4.6. Blood vessels

BVs was observed in 12 (23%) of 51 eyes. There was no quadrant that had significant higher or lower number of BVs than the others and there was no asymmetry between the eyes.

Numerical distribution of gradings for blood vessels (BV) is presented in table 4-6**.** The median and inter quartile range (IQR) per quadrant is presented below each quadrant. Grades are sorted in a descending order. Significant results are marked by *.

			Count of grade, per quadrant (percentage of N)	
Quadrant	**Grade**	**Criteria for grade**	**RE**	**LE**
Inferior	3	Precent in three or all fourths of a quadrant.	0	0
	2	precent in two fourths of a quadrant.	2 (7.7%)	0
	1	Precent	2 (7.7%)	4 (16%)
	0	None	22 (84.6%)	21 (84%)
Median/IQR			0/0	0/0
Temporal	3		0	0
	2		1 (3.9%)	0
	1		3 (11.5%)	1 (4%)
	0		22 (84.6%)	24 (96%)
Median/IQR			0/0	0/0
Superior	3		0	0
	2		0	0
	1		1 (3.9%)	3 (12%)
	0		25 (96.2%)	22 (88%)
Median/IQR			0/0	0/0
Nasal	3		0	0
	2		0	0
	1		2 (7.7%)	2 (8%)
	0		24 (92.3%)	23 (92%)
Median/IQR			0/0	0/0

Table 4-6: numerical distribution of trabecular meshwork pigmentation per quadrant sorted per eye. The Median and interquartile range (IQR) per quadrant is listed below the quadrants.

4.7. Goniosynechia

Goniosynechiae or peripheral anterior synechiae (PAS) was found in 0 eyes. Hence it was not possible to perform any statistically analysis.

5. Discussion

The primary objective was to investigate the visibility of angle structures and gonioscopic findings in four quadrants in young eyes by means of 360-degree goniophotography acquired by the Nidek GS-1 Gonioscope (GS-1).

The GS-1 captured photographs of good quality where the anatomical structures and normal variations was easily identifiable. The most frequent normal variation was trabecular pigmentation, found in 96% of the eyes. There was no significant asymmetry between the eyes for neither image quality, visible anatomical structures of the ACA or any of the normal variations examined. Limitations for the study as a whole are discussed in a separate paragraph. More topic specific limitation is discussed under the relevant subheading.

5.1.Image quality

Out of 204 quadrants photographed, 202 (99%) had the ACA being focused and sufficiently illuminated to distinguish anatomical structures and normal variations. The superior quadrant had the lowest percentage of images with the whole quadrant being in focus and illuminated. There was no significant difference between the eyes.

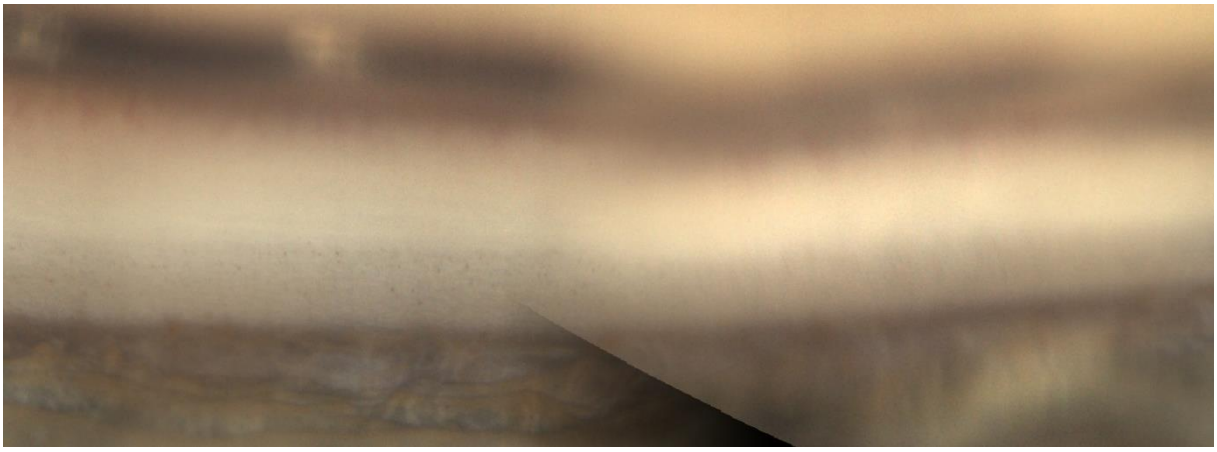

Figure 5-1: example of uneven focus. The focused and unfocused part are imaged trough separate mirrors in the MMP.

In a study using a prototype of the GS-1, Teixeira et. al graded image quality on a 0-2 scale with 0 being the best. On 88 eyes of 47 subjects, only three eyes (3.4%) had good focus and discernible details for 360 degrees, in total 20 (22.7%) of the eyes were excluded due to the ACA structures being difficult/impossible to distinguish. In average only 8 of 16 sectors per eye was graded as the structures being focused with clear details (fig 5-1) (Teixeira et al., 2018). Using the same grading, Matsuo examining 35 patients was excluding an eye if one or more sector per quadrant was graded as no discernible details). He excluded 17 (23.9%) eyes, average grade of IQT for the remaining photographs was 0.33 (Masato Matsuo et al., 2021). Using a slightly modified variant of Teixteira eras grading, Barbour-Hastie et.-al only had to exclude 1 eye of 43. 21 (46%) of the eyes was photographed with the ACA being clear and focused for 360 degrees (Barbour-Hastie et al., 2022). From 84 healthy and glaucomatous eyes, only 28 (8.3%) of 336 quadrants was not gradable in Shis study (Shi et al., 2019). With 99% of the quadrants being gradable, this study found a IQT higher than expected.

There are several possible explanations for why the images of this study scored so high in quality compared to the others. Teixeiras study was performed with an older model of the NGS-1 that had an acquisition time of 2 seconds per image, in total 128 seconds per eye. The other studies mentioned and this, was performed using a newer model were the time of acquisition per image was lower, resulting in a capture time of under 1 minute per eye. The decreased capture time lowers the risk of patients losing

fixation and disturbing the coupling gel. (Nidek, 2018). The GS-1 takes several pictures of varying focal depth per sector. Before compiling the 360-degree goniophotograph, the operator can manually select a picture with a different focal plane than that selected by the GS-1. It is therefore likely that the skill/experience of the operator affects the quality of the final goniophotograph. Teixeiras operator was required by the machine to manually selected the images with best focus, the study was also only grading one image per quadrant. The other studies also performed a manual control before compiling, this study did not. Both Matsuo and Madu found that the clinician having experience in both gonioscopy and goniophotography improved the interobserver repeatability when judging IQT (Madu et al., 2022; Masato Matsuo et al., 2021). This study examined a younger (max age 28 yrs.) population compared with the others. It is possible that clearer corneas improved the IQT.

It was not found any other studies using the GS-1 comparing the bilateral symmetry of IQT or the distribution of quality per quadrant. There are no certain explanations for why the superior quadrant scored lower on the IQT. The MMP is designed to be mounted on the GS-1 with the mirrors in the same orientation each time. There was two different MMPs being used during the study. If one of them had a scratch or opacity on either the lens on the corneal end, on the backside on the MMP facing the camera or on the internal mirrors, this would end up affecting the same areas for each photograph. The coupling gel was applied each time starting on the top of the MMP and ending on the bottom. Some kind of disturbance of the images stemming from the gel in the inferior part is a possible source of the lower IQT. There could also be an innate error in either the camera or the software that had effect only when imaging certain ACA-configurations. The superior quadrant is being imaged through the inferior portion of the MMP. Though unlikely, corneal staining on the inferior parts associated with dry eye could negatively affect the images of the superior quadrant.

The GS-1 captures images of sufficient quality for ACA examination. The superior quadrant had a significantly lower percentage of top rated images than the nasal, inferior and the temporal quadrant. Studies with larger populations and stricter protocols for control of the MMP and gel application of gel is needed. The effect of both the operator acquiring the images and the clinician examining them, on image quality, warrants further research.

5.2.Identifiable angle structures.

Figure 5-2: grade 4 angle opening. Picture of the superior sector as viewed through the MMP. Note the pronounced SL as a white line in the upper half of the image. The SS is barely distinguishable just anterior (above in the image) to the brown CB.

The CB was the most posteriorly visible structure in the majority of the eyes. The inferior quadrant had a significantly narrower angle opening than the superior, nasal and temporal quadrants.

Matsuo et. al. compared manual vs. GS-1 gonioscopy, and the interobserver agreement for angle opening. They found that in average, the SS was the most posterior visible structure (Masato Matsuo et al., 2021). Wang found the CB being visible in 93.7% of preoperative eyes from children with cataracts

(Wang et al., 2022). Phu et. al found that the SS or CB was visible in 56.1%, of patients. They examined an older population of which some had primary angle closure glaucoma. (Phu et al., 2019). Murcia found the SS or CB visible in only 30% of their subjects, average age 50 years (Carrizosa Murcia & Rey Rodríguez, 2019). Campbell et. al found that in 84% of the subjects had non-occludable angles, meaning that at the posterior TM was visible for 270 degrees or more. They did not specify further the most posterior visible structure (Campbell et al., 2015)

Though other studies have examined the ACA opening, this is the first to use the GS-1 for documentation of the distribution. This study was performed on a population of young adults, the oldest subject was 28 years old. Since the ACA opening are known to decrease with age, a wide opening with most of the more posterior structures visible was expected. With the exception of Wang, all the other studies examined an older population of which some had glaucoma. (Shajari et al., 2019). Control of the slit light width and intensity during ordinary gonioscopy is important as stray light entering the pupil cause miosis, affecting the grading of the ACA opening. The light in the MMP is bright and even though the pupil diameter was measured prior to photography, this was not monitored during the procedure. Since absence of stray lighting from the MMP could not be guaranteed, light induced miosis could result in the ACA opening being graded too wide.

The anterior angle was open with the CB being visible in a majority of the eyes. Whether the pupil diameter is affected by the light in the MMP, warrants further research.

5.3.Trabecular meshwork pigmentation

TM pigmentation was found in 96% of the eyes. It was significantly higher in the inferior quadrant than the others (fig.5-3).

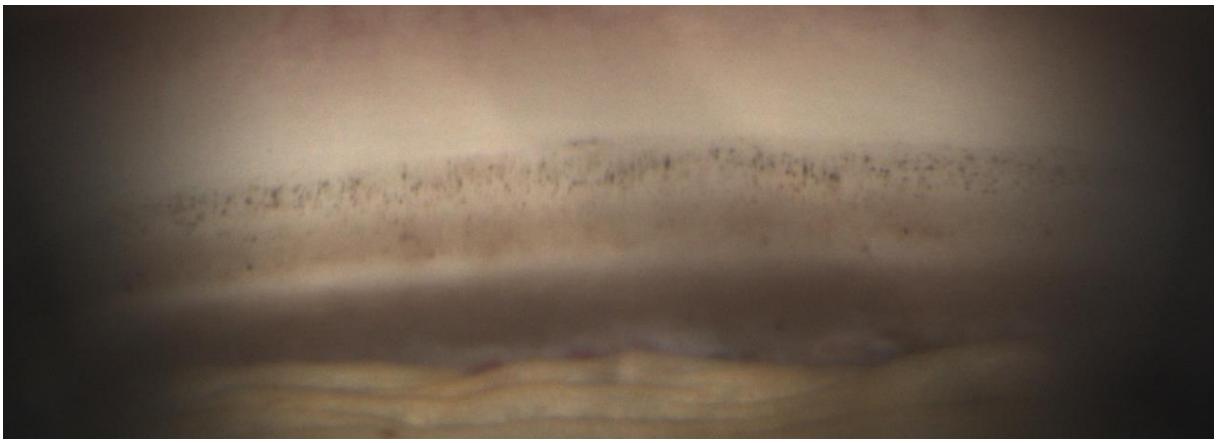

Figure 5-3: grade 3 TM pigmentation from the inferior quadrant.

Research into TM-pigmentation as a normal variation in persons without PDS is limited (Pang et al., 2023). Kimura found with gonioscopy more pigmentation in the inferior followed by the nasal quadrant, and lower in normal versus glaucomatous eyes. They did not record a prevalence (Kimura & Levene, 1975). Wang found TM pigmentation in 64.1% of small children during preoperative examinations using gonioscopy (Wang et al., 2022). Using the GS-1 and grading with a modified Scheies system, Matsuo De Giusti, & Tanito found the inferior quadrant being the more pigmented (M. Matsuo et al., 2019). In a later study, Matsuo et. al again found the inferior quadrant to be the more pigmented. The average Scheie grading of 1.41 for all eyes with the GS-1 was significantly higher than the grading obtained by gonioscopy at 1.13 (Masato Matsuo et al., 2021).

Except Wang, the other studies did not register the prevalence of TM-pigmentation, only graded it and recorded the distribution. This study found a higher prevalence than Wang. Considering that Wangs population was small children, and that TM pigmentation are known to increase into adulthood before

stabilizing, this was expected (Cracknell et al., 2006). In common with the aforementioned studies, this found the inferior quadrant being the more pigmented with similar gradings. As previously mentioned, the majority of AH outflow occurring in the inferior quadrant. Coupled with gravity affecting the pigment particles this makes it an expected result. Due to time constraints and limited experience, gonioscopy was not performed. There is evidence suggesting that clinicians overestimate TM-pigmentation when using goniophotography versus gonioscopy, thus the prevalence can be exaggerated (Masato Matsuo et al., 2021).

An interesting subject worth exploring further are the intra- and interobserver variability comparing goniophotography and gonioscopy. TM pigmentation, its development over time and its association to pigmentation on the corneal posterior surface is highly relevant research.

Trabecular pigmentation was found in almost all of the eyes. The inferior quadrant was significantly more pigmented.

5.4.Iris processes

IPs was found in 86% the eyes. The superior quadrant had a significantly lower number of IPs than the others.

Lichter found IP in 193 (56.7%) of 340 healthy eyes. The majority of these inserted anterior to the SS (Lichter, 1969). Kimura and Levene without recording a prevalence and grading on a 0-3 scale, found a mean grade of 1.82 in 100 healthy subjects. The most IPs was found in the nasal quadrant and then the inferior. They noted the site of insertion and found more insertions in the posterior (CB and SS) parts of the ACA (Kimura & Levene, 1975). Wang found IP in 78.1% of children eyes prior to cataract surgery (Wang et al., 2022).

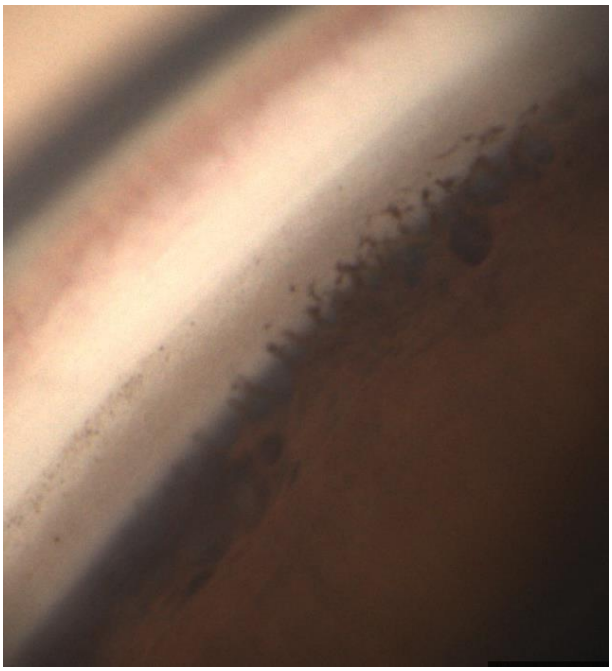

Figure 5-4: Ips inserting into the posterior parts of the TM.

The prevalence if IPs in study was higher than the others but not drastically. One possible explanation is that IPs in blue eyes are easier to overlook because of their lighter colour, making them harder to distinguish from the paler parts of the ACA causing and underestinmation. In fact, Lichter himself states this in his report (Lichter, 1969). However, as previously mentioned goniophotography graded TM-pigmentation higher than gonioscopy. It is possible that a similar overestimation occurred here. Indentation gonioscopy is the most precise method of differentiation IPs from PAS. Because of the inability of the GS-1 to perform this technique, some of the IP could be misclassified PAS inserting posterior of the TM.

There are few studies on the prevalence, distribution and variations of IPs. This study was among the firsts to have used the GS-1 with this intent. Further research into both prevalence, distribution, changes over time and variations of IPs using the GS-1 should be performed. Changes in IPs as a sign of morphological changes in the ACA and its effect on IOP is also interesting for further exploration.

IP was a common finding in the otherwise healthy eyes of this study (fig 5-4).

5.5. Blood vessels

Blood vessels in the ACA was observed in 23% of the eyes with no significant difference between the quadrants or the eyes.

Using gonioscope to examine 269 healthy eyes, Henkind found BVs in the ACA in only 36 (13%) of them (Henkind, 1964). Chatterjee discovered ACA BVs in 65% of healthy eyes. Satoh et. al. was examining leakage from ACA and found ACA-vessels in 28% of otherwise healthy eyes (Chatterjee, 1960; Satoh et al., 1992).

There is not much research available on the prevalence and distribution of physiological BVs in the ACA. Considering the other studies ranging from 13% to 65%, a prevalence of 23% is not unexpected. The majority of subjects in this study was blue eyed. It is theorized that the pigmentation of brown eyes cover up the BVs found in the ACA (Henkind, 1964).

The images captured by the GS-1 lack a depth of focus. This lack of depth made it sometimes difficult to decide whether a BV was located in the ACA or more centrally on the iris. There have been studies using specially developed software to stack the different images per sector, increasing the focal depth of the image (Masato Matsuo et al., 2022). Whether this is

5.6. Goniosynechia

No PAS was discovered during this study.

There is little research describing PAS in healthy eyes without previous trauma or disease/surgery. He et. al. found PAS in 30 (20.5%) of 146 eyes with narrow angles (posterior TM not visible) and in only 7 (0.6%) of 1184 eyes with open angles (He et al., 2006). Excluding eyes with prior history increasing the risk of secondary PAS, Foster et al. found PAS in 4% of 1913 eyes. The prevalence of PAS was greater in quadrants defined as occludable, meaning the posterior TM being visible in less than 90 degrees. In the open angles the prevalence was less than 1.% (Foster et al., 2004)

Examining younger adults without prior disease or injuries and with presumed open angles, the prevalence of PAS was expected to be low or non-existent. As mentioned in the segment about IPs, the most precise way of differentiating PAS from IPs is performing indentation gonioscopy (W. L. M. Alward, 2008). Without gonioscopy, there is a chance that some of the variations classified as IPs actually was PAS only with a more posterior insertion.

Further studies on the formation and prevalence of PAS would be beneficial for the prevention of them.

5.7. Limitations of this study

The most prominent limitation of this study is the low number of subjects. The recruitment of subjects for the project was supposed to take place at USNK in the period august 2020 to January 2022. This was planned as to provide the project manager with time to perform several rounds of recruitment, hopefully ensuring a large number of subjects. Because of covid -19, USNK was partially ,and periodically fully, closed during both the planned and the actual period for recruitment. This left little time, partly explaining the low number of subjects. Lack of blinding was another weakness. Recruitment/scheduling, data collection and the analysis of the images was all done by one person. The last two parts, ideally all three, should have been performed by separate persons. Another weakness of the analysis process is that it was performed one time by one person with limited experience in gonioscopy and goniophotography. As previously mentioned, prior experience in gonioscopy and grading goniophotographs, improves the repeatability in the analysis of the images (Masato Matsuo et al., 2021). Additional experienced observers analysing the photographs in two different, preferably separated by some time, sessions would be beneficial of the precision. Another limitation encountered when grading the quality of images, was the lack of clarification in the scale used. All the studies mentioned, and this, employed different numerical scales when grading IQT but roughly the same criteria. Example of this: for a quadrant to get the best

grading, this study had the criteria “Structures are in focus and sufficiently illuminated in the whole quadrant”. A scale with more precise criteria would eliminate the subjectivity inherent in the grading, increasing precision and repeatability.

6. Conclusion

The GS-1 provided images where the ACA structures was at least partially or fully focused for identification in 99% of the eyes. This makes it a highly suitable instrument for both scientific studies and for clinical use. The ciliary body was visible in 94% of the eyes, the inferior quadrant had the narrowest angle with the ciliary body being visible in 86% of the eyes. Found in 96% of the eyes, trabecular meshwork pigmentation was the most common normal variation with the inferior quadrant being the most pigmented. Iris processes was found in 86% of the eyes. With 78% of the eyes being graded 0 or 1, the superior quadrant had the least IPs. BVs was found in 23% of the eyes without any quadrant differing and no goniosynechiae was found. There was no significant difference between the eyes for image quality, angle opening or prevalence and distribution of the normal variations.

References

Alward, W. L. (2011). A history of gonioscopy. *Optom Vis Sci, 88*(1), 29-35. doi:10.1097/OPX.0b013e3181fc3718

Alward, W. L. M. (2008). *Color atlas of gonioscopy* (2nd ed. ed.). San Francisco: Academy of Ophthalmology.

Ansari, M. W., & Nadeem, A. (2016). The Blood Supply to the Eyeball. In (pp. 29-38). Switzerland: Switzerland: Springer International Publishing AG.

Ascher, K. (1942). Aqueous veins: preliminary note. *Am J Ophthalmol, 25*(1), 31-38.

Barbour-Hastie, C., Deol, S. S., Peroni, A., Gillan, S., Trucco, E., & Tatham, A. J. (2022). Feasibility of Automated Gonioscopy Imaging in Clinical Practice. *J Glaucoma*, 10.1097/IJG.0000000000002162. doi:10.1097/ijg.0000000000002162

Bill, A. (1965). The aqueous humor drainage mechanism in the cynomolgus monkey (Macaca irus) with evidence for unconventional routes. *Invest Ophthalmol, 4*(5), 911-919.

Boote, C., Sigal, I. A., Grytz, R., Hua, Y., Nguyen, T. D., & Girard, M. J. A. (2020). Scleral structure and biomechanics. *Prog Retin Eye Res, 74*, 100773. doi:10.1016/j.preteyeres.2019.100773

Breazzano, M. P., Fikhman, M., Abraham, J. L., & Barker-Griffith, A. E. (2013). Analysis of Schwalbe's Line (Limbal Smooth Zone) by Scanning Electron Microscopy and Optical Coherence Tomography in Human Eye Bank Eyes. *J Ophthalmic Vis Res, 8*(1), 9-16.

Campbell, P., Redmond, T., Agarwal, R., Marshall, L. R., & Evans, B. J. (2015). Repeatability and comparison of clinical techniques for anterior chamber angle assessment. *Ophthalmic Physiol Opt, 35*(2), 170-178. doi:10.1111/opo.12200

Carrizosa Murcia, M., & Rey Rodríguez, D. V. (2019). Evaluation of the angle of the anterior chamber using ultrasound biomicroscopy, gonioscopy and a Van Herick examination. *Arch Soc Esp Oftalmol (Engl Ed), 94*(3), 114-118. doi:10.1016/j.oftal.2018.09.011

Cha, E. D. K., Xu, J., Gong, L., & Gong, H. (2016). Variations in active outflow along the trabecular outflow pathway. *Experimental Eye Research, 146*, 354-360. doi:https://doi.org/10.1016/j.exer.2016.01.008

Chatterjee, S. (1960). Gonio-vessels in normal and abnormal eyes. *Br J Ophthalmol, 44*(6), 347-352. doi:10.1136/bjo.44.6.347

Cheuk, B. S., Kumar, A., & Du, Y. (2022). Chapter 3 - Induced pluripotent stem cells for modeling open-angle glaucoma. In A. Birbrair (Ed.), *Novel Concepts in iPSC Disease Modeling* (Vol. 15, pp. 85-104): Academic Press.

Costagliola, C., dell’Omo, R., Agnifili, L., Bartollino, S., Fea, A. M., Uva, M. G., . . . Mastropasqua, L. (2020). How many aqueous humor outflow pathways are there? *Surv Ophthalmol, 65*(2), 144-170. doi:https://doi.org/10.1016/j.survophthal.2019.10.002

Coulon, S. J., Schuman, J. S., Du, Y., Bahrani Fard, M. R., Ethier, C. R., & Stamer, W. D. (2022). A novel glaucoma approach: Stem cell regeneration of the trabecular meshwork. *Prog Retin Eye Res, 90*, 101063. doi:https://doi.org/10.1016/j.preteyeres.2022.101063

Cracknell, K. P. B., Grierson, I., Hogg, P., Majekodunmi, A. A., Watson, P., & Marmion, V. (2006). Melanin in the trabecular meshwork is associated with age, POAG but not Latanoprost treatment. A masked morphometric study. *Experimental Eye Research, 82*(6), 986-993. doi:https://doi.org/10.1016/j.exer.2005.10.009

Cutolo, C. A., Bonzano, C., Scotto, R., Iester, M., Bagnis, A., Pizzorno, C., . . . Traverso, C. E. (2021). Moving beyond the Slit-Lamp Gonioscopy: Challenges and Future Opportunities. *Diagnostics (Basel), 11*(12). doi:10.3390/diagnostics11122279

Doane, J. F., Rickstrew, J. J., Tuckfield, J. Q., & Cauble, J. E. (2019). Prevalence of Pigment Dispersion Syndrome in Patients Seeking Refractive Surgery. *J Glaucoma, 28*(5), 423-426. doi:10.1097/ijg.0000000000001193

felleskatalogen.no. (2023, 20.03.2019). Oxibuprokain Minims. Retrieved from https://www.felleskatalogen.no/medisin/oxibuprokain-minims-bausch-health-562535?freeTextSearch=true

Fernández-Vigo, J. I., Kudsieh, B., Shi, H., De-Pablo-Gómez-de-Liaño, L., Fernández-Vigo, J., & García-Feijóo, J. (2022). Diagnostic imaging of the ciliary body: Technologies, outcomes, and future perspectives. *Eur J Ophthalmol, 32*(1), 75-88. doi:10.1177/11206721211031409

Foster, P. J., Aung, T., Nolan, W. P., Machin, D., Baasanhu, J., Khaw, P. T., . . . Johnson, G. J. (2004). Defining "occludable" angles in population surveys: drainage angle width, peripheral anterior synechiae, and glaucomatous optic neuropathy in east Asian people. *Br J Ophthalmol, 88*(4), 486-490. doi:10.1136/bjo.2003.020016

Friedman, D. S., & He, M. (2008). Anterior chamber angle assessment techniques. *Surv Ophthalmol, 53*(3), 250-273. doi:10.1016/j.survophthal.2007.10.012

Garcia, J. P., Jr., Spielberg, L., & Finger, P. T. (2011). High-frequency ultrasound measurements of the normal ciliary body and iris. *Ophthalmic Surg Lasers Imaging, 42*(4), 321-327. doi:10.3928/15428877-20110603-03

Gasiorowski, J. Z., & Russell, P. (2009). Biological properties of trabecular meshwork cells. *Exp Eye Res, 88*(4), 671-675. doi:10.1016/j.exer.2008.08.006

Gaton, D., Barak, A., Segev, S., Yassur, Y., & Treister, G. (1998). [Prevalence of pigmentary dispersion syndrome in Israel]. *Harefuah, 134*(5), 337-339, 424.

Giusti, A., Pajaro, S., & Tanito, M. (2018). Automatic Pigmentation Grading of the Trabecular Meshwork in Gonioscopic Images: First International Workshop, COMPAY 2018, and 5th International Workshop, OMIA 2018, Held in Conjunction with MICCAI 2018, Granada, Spain, September 16 - 20, 2018, Proceedings. In (pp. 193-200).

Gong, J. L., Al-Wesabi, S. A., Zhao, Y., & Zhang, H. (2018). Positive correlation between blood reflux in Schlemm's canal and the decrease of intraocular pressure after selective laser trabeculoplasty in primary open-angle glaucoma. *Exp Ther Med, 15*(6), 5065-5069. doi:10.3892/etm.2018.6051

Grieshaber, M. C., Pienaar, A., Olivier, J., & Stegmann, R. (2010). Clinical evaluation of the aqueous outflow system in primary open-angle glaucoma for canaloplasty. *Invest Ophthalmol Vis Sci, 51*(3), 1498-1504. doi:10.1167/iovs.09-4327

He, M., Foster, P. J., Ge, J., Huang, W., Wang, D., Friedman, D. S., & Khaw, P. T. (2006). Gonioscopy in adult Chinese: the Liwan Eye Study. *Invest Ophthalmol Vis Sci, 47*(11), 4772-4779. doi:10.1167/iovs.06-0309

Henkind, P. (1964). ANGLE VESSELS IN NORMAL EYES. A GONIOSCOPIC EVALUATION AND ANATOMIC CORRELATION. *Br J Ophthalmol, 48*, 551-557. doi:10.1136/bjo.48.10.551

Jain, N., & Zia, R. (2021). The prevalence and break down of narrow anterior chamber angle pathology presenting to a general ophthalmology clinic. *Medicine (Baltimore), 100*(24), e26195. doi:10.1097/md.0000000000026195

Johnson, M., McLaren, J. W., & Overby, D. R. (2017). Unconventional aqueous humor outflow: A review. *Exp Eye Res, 158*, 94-111. doi:10.1016/j.exer.2016.01.017

Kanski, J. J. (2007). *Clinical ophthalmology, a systematic approach*: Butterworth Heineman Elsevier.

Keller, K. E., & Peters, D. M. (2022). Pathogenesis of glaucoma: Extracellular matrix dysfunction in the trabecular meshwork-A review. *Clin Exp Ophthalmol, 50*(2), 163-182. doi:10.1111/ceo.14027

Kimura, R., & Levene, R. Z. (1975). Gonioscopic differences between eyes with primary open-angle glaucoma and normal eyes in subjects over the age of forty. *Trans Am Ophthalmol Soc, 73*, 74-85.

Laroche, D., Rickford, K., Sinon, J., Brown, A., Ng, C., & Sakkari, S. (2023). Preventing blindness from glaucoma with patient education, the NIDEK GS-1 Gonioscope, lensectomy and microinvasive glaucoma surgery. *J Natl Med Assoc*. doi:10.1016/j.jnma.2023.01.014

Lee, J. Y., Kim, Y. Y., & Jung, H. R. (2006). Distribution and characteristics of peripheral anterior synechiae in primary angle-closure glaucoma. *Korean J Ophthalmol, 20*(2), 104-108. doi:10.3341/kjo.2006.20.2.104

Lee, R. Y., Lin, S.-C., Chen, R. I., Barbosa, D. T., & Lin, S. C. (2016). Association between light-to-dark changes in angle width and iris parameters in light, dark and changes from light-to-dark conditions. *British Journal of Ophthalmology, 100*(9), 1274-1279. doi:10.1136/bjophthalmol-2015-307393

Lee, T. E., Yoo, C., & Kim, Y. Y. (2021). The effects of peripheral anterior synechiae on refractive outcomes after cataract surgery in eyes with primary angle-closure disease. *Medicine (Baltimore), 100*(14), e24673. doi:10.1097/md.0000000000024673

Li, M., Luo, Z., Yan, X., & Zhang, H. (2020). Diagnostic power of scleral spur length in primary open-angle glaucoma. *Graefe's Archive for Clinical and Experimental Ophthalmology, 258*(6), 1253-1260. doi:10.1007/s00417-020-04637-4

Lichter, P. R. (1969). Iris Processes in 340 Eyes. *Am J Ophthalmol, 68*(5), 872-878. doi:10.1016/0002-9394(69)94583-8

Madu, C. T., Phelps, T., Schuman, J. S., Zambrano, R., Lee, T.-F., Panarelli, J., . . . Wollstein, G. (2022). Automated 360-degree goniophotography with the NIDEK Gonioscope GS-1 for glaucoma. *medRxiv*, 2022.2006.2022.22276741. doi:10.1101/2022.06.22.22276741

Malihi, M., & Sit, A. J. (2011). Aqueous humor dynamics and implications for clinical practice. *Int Ophthalmol Clin, 51*(3), 119-139. doi:10.1097/IIO.0b013e31821e5cea

Matsuo, M., Kozuki, N., Inomata, Y., Kumagai, Y., Shiba, R., Hamaguchi, K., & Tanito, M. (2022). Automated Focal Plane Merging From a Stack of Gonioscopic Photographs Using a Focus-Stacking Algorithm. *Transl Vis Sci Technol, 11*(4), 22-22. doi:10.1167/tvst.11.4.22

Matsuo, M., Mizoue, S., Nitta, K., Takai, Y., Sugihara, K., & Tanito, M. (2021). Intraobserver and interobserver agreement among anterior chamber angle evaluations using automated 360-degree gonio-photos. *PLOS ONE, 16*(5), e0251249. doi:10.1371/journal.pone.0251249

Matsuo, M., Pajaro, S., De Giusti, A., & Tanito, M. (2019). Automated anterior chamber angle pigmentation analyses using 360 degrees gonioscopy. *Br J Ophthalmol*. doi:10.1136/bjophthalmol-2019-314320

Matsuo, M., Pajaro, S., De Giusti, A., & Tanito, M. (2020). Automated anterior chamber angle pigmentation analyses using 360° gonioscopy. *British Journal of Ophthalmology, 104*(5), 636-641. doi:10.1136/bjophthalmol-2019-314320

McGowan, S. L., Edelhauser, H. F., Pfister, R. R., & Whikehart, D. R. (2007). Stem cell markers in the human posterior limbus and corneal endothelium of unwounded and wounded corneas. *Mol Vis, 13*, 1984-2000.

Nidek. (2018, 20-09-2018). NIDEK launches the GS-1 Gonioscope.

Pang, R., Labisi, S. A., & Wang, N. (2023). Pigment dispersion syndrome and pigmentary glaucoma: overview and racial disparities. *Graefe's Archive for Clinical and Experimental Ophthalmology, 261*(3), 601-614. doi:10.1007/s00417-022-05817-0

Perera, S. A., Baskaran, M., Friedman, D. S., Tun, T. A., Htoon, H. M., Kumar, R. S., & Aung, T. (2010). Use of EyeCam for imaging the anterior chamber angle. *Invest Ophthalmol Vis Sci, 51*(6), 2993-2997. doi:10.1167/iovs.09-4418

Phu, J., Wang, H., Khou, V., Zhang, S., & Kalloniatis, M. (2019). Remote Grading of the Anterior Chamber Angle Using Goniophotographs and Optical Coherence Tomography: Implications for Telemedicine or Virtual Clinics. *Transl Vis Sci Technol, 8*(5), 16. doi:10.1167/tvst.8.5.16

Pineles, S. L., Chang, M. Y., Oltra, E. L., Pihlblad, M. S., Davila-Gonzalez, J. P., Sauer, T. C., & Velez, F. G. (2018). Anterior segment ischemia: etiology, assessment, and management. *Eye, 32*(2), 173-178. doi:10.1038/eye.2017.248

Porporato, N., Baskaran, M., Husain, R., & Aung, T. (2020). Recent advances in anterior chamber angle imaging. *Eye, 34*(1), 51-59. doi:10.1038/s41433-019-0655-0

Raluca, M., Mircea, F., Andrei, F., Carmen, D., Miruna, N., Grigorios, T., & Ileana, U. (2015). Old and new in exploring the anterior chamber angle. *Rom J Ophthalmol, 59*(4), 208-216.

Sakata, L. M., Lavanya, R., Friedman, D. S., Aung, H. T., Gao, H., Kumar, R. S., . . . Aung, T. (2008). Comparison of gonioscopy and anterior segment ocular coherence tomography in detecting angle closure in different quadrants of the anterior chamber angle. *Ophthalmology, 115*(5), 769-774. doi:10.1016/j.ophtha.2007.06.030

Satoh, K., Takaku, Y., Ohtsuki, K., & Mizuno, K. (1999). Effects of aging on fluorescein leakage in the iris and angle in normal subjects. *Jpn J Ophthalmol, 43*(3), 166-170. doi:10.1016/s0021-5155(99)00012-x

Satoh, K., Takaku, Y., Ootsuki, K., & Mizuno, K. (1992). [Effects of aging on fluorescein iris and angle photography in normal subjects]. *Nippon Ganka Gakkai Zasshi, 96*(5), 657-663.

Scheie, H. G. (1957). Width and pigmentation of the angle of the anterior chamber; a system of grading by gonioscopy. *AMA Arch Ophthalmol, 58*(4), 510-512. doi:10.1001/archopht.1957.00940010526005

Schuster, A. K., Pfeiffer, N., Nickels, S., Schulz, A., Höhn, R., Wild, P. S., . . . Vossmerbaeumer, U. (2016). Distribution of Anterior Chamber Angle Width and Correlation With Age, Refraction, and Anterior Chamber Depth-The Gutenberg Health Study. *Invest Ophthalmol Vis Sci, 57*(8), 3740-3746. doi:10.1167/iovs.16-19600

Seidel, E. (1921). Weitere experimentelle Untersuchungen über die Quelle und den Verlauf der intraokularen Saftströmung: IX. Mitteilung. Über den Abfluß des Kammerwassers aus der vorderen Augenkammer. *Albrecht von Graefes Archiv für Ophthalmologie, 104*, 357-402.

Shaffer, R. N. (1960). Primary glaucomas. Gonioscopy, ophthalmoscopy and perimetry. *Trans Am Acad Ophthalmol Otolaryngol, 64*, 112-127.

Shajari, M., Herrmann, K., Bühren, J., Vunnava, P., Vounotrypidis, E., Müller, M., . . . Kohnen, T. (2019). Anterior Chamber Angle, Volume, and Depth in a Normative Cohort-A Retrospective Cross-Sectional Study. *Curr Eye Res, 44*(6), 632-637. doi:10.1080/02713683.2019.1576205

Shi, Y., Yang, X., Marion, K. M., Francis, B. A., Sadda, S. R., & Chopra, V. (2019). Novel and Semiautomated 360-Degree Gonioscopic Anterior Chamber Angle Imaging in Under 60 Seconds. *Ophthalmol Glaucoma, 2*(4), 215-223. doi:10.1016/j.ogla.2019.04.002

Sie, N. M., Yam, G. H.-F., Soh, Y. Q., Lovatt, M., Dhaliwal, D., Kocaba, V., & Mehta, J. S. (2020). Regenerative capacity of the corneal transition zone for endothelial cell therapy. *Stem Cell Research & Therapy, 11*(1), 523. doi:10.1186/s13287-020-02046-2

Spaeth, G. L. (1971). The normal development of the human anterior chamber angle: a new system of descriptive grading. *Trans Ophthalmol Soc U K, 91*, 709-739.

Spencer, W. H., Alvarado, J., & Hayes, T. L. (1968). Scanning electron microscopy of human ocular tissues: trabecular meshwork. *Invest Ophthalmol, 7*(6), 651-662.

Srinivas, S. P., Guidoboni, G., Burli, A., Harjai, B., & Kompella, U. B. (2021). Anatomy and Physiology of the Anterior Chamber: Impact on Product Development. In S. Neervannan & U. B. Kompella (Eds.), *Ophthalmic Product Development: From Bench to Bedside* (pp. 39-64). Cham: Springer International Publishing.

Stamer, W. D., & Clark, A. F. (2017). The many faces of the trabecular meshwork cell. *Exp Eye Res, 158*, 112-123. doi:10.1016/j.exer.2016.07.009

Stamper, R. L., Lieberman, M. F., & Drake, M. V. (2009). CHAPTER 2 - Aqueous humor formation. In R. L. Stamper, M. F. Lieberman, & M. V. Drake (Eds.), *Becker-Shaffer's Diagnosis and Therapy of the Glaucomas (Eighth Edition)* (pp. 8-24). Edinburgh: Mosby.

Tamm, E., Flügel, C., Stefani, F. H., & Rohen, J. W. (1992). Contractile cells in the human scleral spur. *Exp Eye Res, 54*(4), 531-543. doi:10.1016/0014-4835(92)90132-c

Tamm, E. R. (2009). The trabecular meshwork outflow pathways: structural and functional aspects. *Exp Eye Res, 88*(4), 648-655. doi:10.1016/j.exer.2009.02.007

Tandon, A., & Alward, W. L. M. (2015). The Centennial of Modern Gonioscopy. *Ophthalmologica, 233*(1), 58-59. doi:10.1159/000365789

Teixeira, F., Sousa, D. C., Leal, I., Barata, A., Neves, C. M., & Pinto, L. A. (2018). Automated gonioscopy photography for iridocorneal angle grading. *Eur J Ophthalmol*, 1120672118806436. doi:10.1177/1120672118806436

Toris, C. B., Yablonski, M. E., Wang, Y. L., & Camras, C. B. (1999). Aqueous humor dynamics in the aging human eye. *Am J Ophthalmol, 127*(4), 407-412. doi:10.1016/s0002-9394(98)00436-x

Van Herick, W., Shaffer, R. N., & Schwartz, A. (1969). Estimation of width of angle of anterior chamber. Incidence and significance of the narrow angle. *Am J Ophthalmol, 68*(4), 626-629. doi:10.1016/0002-9394(69)91241-0

Vossmerbaeumer, U., Schuster, A. K., & Fischer, J. E. (2013). Width of anterior chamber angle determined by OCT, and correlation to refraction and age in a German working population: the MIPH Eye&Health Study. *Graefes Arch Clin Exp Ophthalmol, 251*(12), 2741-2746. doi:10.1007/s00417-013-2472-7

Wang, D. D., Li, Z. L., Zhang, B., Lu, Z. Y., Guan, W. C., & Zhao, Y. E. (2022). Morphological changes in the iridocorneal angle and their relationship with intraocular pressure after infantile cataract surgery. *Int J Ophthalmol, 15*(9), 1453-1459. doi:10.18240/ijo.2022.09.07

Whikehart, D. R., Parikh, C. H., Vaughn, A. V., Mishler, K., & Edelhauser, H. F. (2005). Evidence suggesting the existence of stem cells for the human corneal endothelium. *Mol Vis, 11*, 816-824.
Wolff, E., Bron, A. J., Tripathi, R. C., & Tripathi, B. J. (1997). *Wolff's anatomy of the eye and orbit*. London; Weinheim; Tokyo: Chapman & Hall medical.
WuDunn, D. (2009). Mechanobiology of trabecular meshwork cells. *Exp Eye Res, 88*(4), 718-723. doi:10.1016/j.exer.2008.11.008
Yucel, Y., & Gupta, N. (2015). Chapter 9 - Lymphatic drainage from the eye: A new target for therapy. In G. Bagetta & C. Nucci (Eds.), *Progress in Brain Research* (Vol. 220, pp. 185-198): Elsevier.

List of figures and tables.

Annexes

Annex 1: consent form (in Norwegian)

Annex 2: Registration form

Annex 3: Flyer for recruitment.

Annex 1: Consent form

FORESPØRSEL OM DELTAKELSE I FORSKNINGSPROSJEKTET

Distribusjon av gonioskopiske funn på goniofotografier av unge voksne tatt med Nidek GS-1 Gonioscop

Kammervinkelen er en struktur i øyets fremre del som spiller en viktig rolle i opprettholdelsen av øyets trykk. Den vanligste måten å undersøke kammervinkelen hos optiker eller øyelege er ved hjelp av et kontaktglass som legges mot øyet etter en dråpe med bedøvelse. Metoden som kalles gonioskopi krever mye trening av den som utfører undersøkelsen, både med hensyn til håndteringen av kontaktglasset og med hensyn til tolkningen av det man ser. I tillegg er det ofte utfordrende å fotografere funn gjennom kontaktglasset. I mange sammenhenger hadde det vært ønskelig å kunne undersøke kammervinkelen og dokumentere funn på en måte som ikke er så avhengig av undersøkelsens ferdigheter og erfaring som ved gonioskopi med kontaktglass. Nidek GS-1 Gonioscope er et nytt instrument for fotografering av kammervinkelen som gir denne muligheten.

Dette er et spørsmål til deg om å delta i et forskningsprosjekt ved Nasjonalt senter for optikk, syn og øyehelse, Universitetet i Sør-øst Norge, Campus Kongsberg. Formålet med prosjektet er å kartlegge hvilke variasjoner i øyets kammervinkel man kan finne ved bruk av et Nidek GS-1 Gonioscope i en gruppe med unge personer. Dette vil gi kunnskap om normalvariasjoner i kammervinkelen og erfaringer i bruken av en ny klinisk undersøkelsesmetode som eventuelt kan erstatte kontaktglasset som førstevalg for undersøkelse av øyets kammervinkel. Du har blitt forespurt om deltagelse fordi du som student ved USN, tilhører en gruppe unge personer som ofte befinner deg på Campus Kongsberg. Invitasjonen har vært distribuert via sosiale medier og oppslag på USN, Campus Kongsberg.

HVA INNEBÆRER PROSJEKTET?

Det blir avtalt tid til en kort forundersøkelse og fotografering av kammervinkelen i høyre og venstre øye med Nidek GS-1 Gonioscope. Hele prosedyren tar ca 30 minutter. Forundersøkelsen innebærer at du besvarer noen spørsmål om øyehelsen din før enkle målinger av brillestyrke, trykk, hornhinnens krumming og tykkelse foretas. Deretter får du en dråpe bedøvelse i hvert øye og får sette deg bak et kamera med en spesiell linse som gjør det mulig å fotografere kammervinkelen. Det legges en klikk gel på linsen som deretter legges lett på øyet. Det vil bli tatt flere bilder for å sikre at billedkvaliteten blir så god som mulig. Etter ca 30 minutter har øyet fått tilbake normal følsomhet. Synet påvirkes ikke av undersøkelsen slik at du kan gå tilbake til normal aktivitet etter undersøkelsen. Dersom du bruker kontaktlinser vil du få muligheter å ta ut disse og oppbevare de i saltvann under undersøkelsen. Kontaktlinsene kan tas på igjen når følsomheten i øyet er tilbake.

Undersøkelsen tar ca. 30 minutter totalt.

I prosjektet vil vi innhente og registrere opplysninger om deg. Disse opplysningene omhandler alder, brillestyrker, hornhinnens krumning, øyetrykket samt historikk om skader på øynene, øyesykdommer og systemiske sykdommer. Resultatene av målingene registreres i et skjema hvor ditt navn er erstattet med et ID nummer. ID nummeret kobles til ditt navn ved hjelp av en nøkkel som oppbevares adskilt fra informasjonen som samles inn. Bildene som tas blir lagret på en kryptert harddisk under samme ID nummer. Nøkkelen som kobler navn til ID nummer slettes 5 år etter prosjektets fullførelse i samsvar med Regional Etisk Komite sine regler. Seneste dato for sletting er 30. juni 2028.

MULIGE FORDELER OG ULEMPER

Det er ingen direkte fordeler eller ulemper forent med deltakelse i prosjektet. Dråpene som blir brukt for å bedøve øyne i prosjektet er Oxibuprocain 0,4%. Disse dråpene gir forbigående svie ved påføring og i sjeldne tilfeller kortvarig tåkesyn. En kraftigere allergisk reaksjon kan forekomme men det er veldig uvanlig. Størrelsen på pupillene blir ikke påvirket. Gelen som legges på linsen kan årsake lett slørsyn i en kort periode etter fotograferingen. Det er ingen andre risikoer forbundet med gelen. Hvert bilde tar ca. 1 minutt. Når bildet taes sveipes et skarpt lys mot fremre del av øyet, dette kan oppfattes som svakt sjenerende.

FRIVILLIG DELTAKELSE OG MULIGHET FOR Å TREKKE SITT SAMTYKKE

Det er frivillig å delta i prosjektet. Dersom du ønsker å delta, undertegner du samtykkeerklæringen på siste side. Du kan når som helst og uten å oppgi noen grunn trekke ditt samtykke. Dersom du trekker deg fra prosjektet, kan du kreve å få slettet innsamlede prøver og opplysninger, med mindre opplysningene allerede er inngått i analyser eller brukt i vitenskapelige publikasjoner. Dersom du senere ønsker å trekke deg eller har spørsmål til prosjektet, kan du kontakte Per O. Lundmark, e-post per.lundmark@usn.no, tel. 31 00 89 37 eller prosjektmedarbeider Kristian Brekstad, kristian.brekstad@gmail.com, mob. 95 24 21 38.

HVA SKJER MED OPPLYSNINGENE OM DEG?

Opplysningene som registreres om deg skal kun brukes slik som beskrevet i hensikten med prosjektet. Du har rett til innsyn i hvilke opplysninger som er registrert om deg og rett til å få korrigert eventuelle feil i de opplysningene som er registrert. Du har også rett til å få innsyn i sikkerhetstiltakene ved behandling av opplysningene.

Alle opplysningene vil bli behandlet uten navn og fødselsnummer eller andre direkte gjenkjennende opplysninger. En kode knytter deg til dine opplysninger gjennom en navneliste. Det er kun Per O. Lundmark og Kristian Brekstad som har tilgang til denne listen.

FORSIKRING

Alle deltakere i prosjektet er dekket av pasientskadeerstatningsordningen.

GODKJENNING

Regional komité for medisinsk og helsefaglig forskningsetikk har vurdert prosjektet, og har gitt forhåndsgodkjenning. SøknadsID 119826, 2020.

Etter ny personopplysningslov har behandlingsansvarlig institusjon Universitetet i Sørøst-Norge og prosjektleder Per O. Lundmark et selvstendig ansvar for å sikre at behandlingen av dine opplysninger har et lovlig grunnlag. Dette prosjektet har rettslig grunnlag i EUs personvernforordning artikkel 6 nr. 1a og artikkel 9 nr. 2a og ditt samtykke.

Du har rett til å klage på behandlingen av dine opplysninger til Datatilsynet.

KONTAKTOPPLYSNINGER

Dersom du har spørsmål til prosjektet kan du ta kontakt med prosjektmedarbeider Kristian Brekstad, e-post kristian.brekstad@gmail.com, mobil 95 24 21 38, eller prosjektansvarlig Per O. Lundmark, e-post per.lundmark@usn.no, tel. 31 00 89 37. Personvernombud ved Universitetet i Sørøst-Norge er Paal Are Solberg, e-post paal.a.solberg@usn.no, tlf 35 57 50 53/918 60 041.

JEG SAMTYKKER TIL Å DELTA I PROSJEKTET OG TIL AT MINE PERSONOPPLYSNINGER BRUKES SLIK DET ER BESKREVET

Sted og dato

Deltakers signatur

Deltakers navn med trykte bokstaver

Jeg bekrefter å ha gitt informasjon om prosjektet

Sted og dato

Signatur

Prosjekmedarbeider

Rolle i prosjektet

Annex 2 Data registration form

Patient ID	Age	Gender	Systemic pathology	CCT	IOP	Keratometry	Pupil size	Refraction	Previous trauma	Eye colour	IQ Superior	IQ temporal	IQ inferior	IQ nasal	AAS Superior	AAS temporal	AAS inferior	AAS nasal	TP Superior	TP temporal	TP inferior	TP nasal	IP Superior	IP temporal	IP inferior	IP nasal	BV Superior	BV temporal	BV inferior	BV nasal	GS superior	GS temporal	GS inferior	GS nasal
ID1			OD	550		22.6;3.50@140	11	-1.75		0 Blue																								
ID1	28	1	OS	548		21.6;7.00@	10	-1.35		0 Blue	2	1	1	1	4	4	4	4	0	1	1	0	1	1	0	2	1	0	0	1	0	0	0	1
ID2			OD	520		16.8;0.00@24	8	3.25		0 Blue	2	1	1	1	4	4	4	4	0	1	2	0	0	1	2	0	0	1	0	0	0	0	0	0	1
ID2	19	1	OS	538		16.4;0.00@33	8	3.75		0 Blue	2	1	1	1	4	4	4	4	0	1	2	0	0	1	1	0	1	1	1	1	0	0	0	1
ID3			OD	584		17.7;6.00@179	9	-1		0 Brown	1	1	1	1	4	4	4	3	4	1	2	0	3	3	3	3	0	0	0	0	0	0	1	0
ID3	29	1	OS	588		19.7;5.00@	8	-0.25		0 Brown	2	1	1	1	4	4	4	3	3	0	0	1	3	3	3	3	2	0	0	0	0	1	1	1
ID6			OD	508		18.7;4.00@177	10	4.5		0 Blue	1	1	1	1	4	4	4	4	0	1	1	0	1	1	0	0	0	0	0	0	0	0	0	0	0
ID6	29	1	OS	505		19.7;4.00@5	11	4		0 Blue	1	1	1	1	4	4	4	4	0	1	0	1	0	0	1	0	0	0	0	1	0	0	0	0
ID7			OD	543		11.7;6.00@16	7	0		0 Blue	1	1	1	1	4	4	4	4	0	1	2	0	0	0	0	0	0	0	0	0	0	0	0	0
ID7	30	1	OS	530		10.7;5.00@1	8	-0.5		0 Blue	2	1	1	1	4	4	4	4	0	0	2	0	0	0	0	0	1	0	0	1	0	0	1	0
ID8			OD	553		13.7;5.00@177	7.5	1.25		0 Green	1	1	1	1	4	4	4	4	0	1	1	0	1	1	0	0	1	0	0	0	0	0	0	0
ID8	32	1	OS	550		15.7;6.00@171	8	1.25		0 Green	1	1	1	1	4	4	4	4	1	0	2	1	2	1	2	3	3	0	0	0	0	0	0	0
ID9			OD	538		13.8;1.75@157	9	-0.25		0 Blue	1	1	1	1	4	4	4	4	0	0	2	0	3	2	1	2	1	0	2	0	0	0	0	0	0
ID9	22	0	OS	514		12.8;0.00@17	9	0		0 Blue	1	2	0	0	4	4	4	4	0	0	2	1	2	1	1	2	0	0	1	0	0	0	0	0
ID10			OD	610		20.7;3.00@175	8.5	-1.5		0 Blue	1	1	2	1	4	4	3	4	0	0	1	0	0	0	0	0	0	0	0	0	0	0	0	0
ID10	23	0	OS	611		21.7;3.00@118	7.5	-1.5		0 Blue	3	3	3	0	4	4	4	4	0	0	1	0	0	0	0	0	0	0	0	0	0	0	0	0
ID11			OD	558		13.7;3.00@7	8	1.5		0 Green	1	1	1	1	4	4	4	4	1	0	2	0	2	2	3	2	0	0	0	0	0	0	0	0
ID11	27	0	OS	580		16.7;3.00@175	8	1.25		0 Green	1	1	1	1	4	4	4	4	0	0	1	0	0	1	2	2	0	0	0	0	0	0	0	0
ID12			OD	623		28.7;5.00@164	10.5	0.25		1	1	2	1	1	4	4	4	4	1	1	1	0	1	1	0	1	0	0	0	0	0	0	0	0
ID12	26	1	OS	611		25.7;4.00@13	10	0.25		1	1	1	1	1	4	4	4	4	0	0	1	0	1	1	1	1	0	0	0	0	0	0	0	1
ID13			OD	575		15.7;8.47@108	8.5	0.25		0 Brown	1	1	1	1	4	4	3	4	1	1	2	1	1	1	2	2	0	0	0	0	0	0	0	1
ID13	22	1	OS	592		17.7;6.00@4	9.5	0.5		0 Brown	2	1	1	1	4	4	4	3	4	1	2	1	1	1	3	2	0	0	0	0	1	1	1	0
ID15			OD	500		12.7;9.17@184	11	0.25		0	1	1	1	1	4	4	4	4	0	0	2	0	0	1	2	1	0	0	1	0	0	0	0	0	0
ID15	31	0	OS	501		12.7;8.17@184	11	-0.25		0	2	2	1	1	4	4	4	4	0	0	1	0	1	2	1	1	0	0	1	0	0	0	0	0	0
ID18			OD	539		12.7;9.17@4E	8	0.25		0 Blue	1	1	1	1	4	4	4	4	0	0	1	0	0	0	1	1	0	0	0	0	0	0	0	0	0
ID18	21	0	OS	530		13.7;9.17@15E	8.5	0.25		0 Blue	1	1	1	1	4	4	4	4	0	0	1	0	1	0	1	0	0	0	0	0	0	0	0	0
ID19			OD	551		14.7;9.17@19E	7	0.5		0 Blue	2	1	1	1	4	4	3	4	0	0	1	0	0	1	0	0	0	0	0	0	0	0	1	0
ID19	26	1	OS	560		14.7;9.17@5E	8	0.5		0 Blue	1	1	1	1	4	4	4	4	0	0	1	0	0	1	0	0	0	0	0	0	0	0	1	1
ID20			OD	528		14.7;9.17@76E	6	-3.75		0 Brown	1	1	1	1	4	4	4	4	1	1	2	1	2	1	1	2	0	0	0	0	0	0	0	0
ID20	25	1	OS	528		14.7;9.17@7.5E	6.5	-3.5		0 Brown	1	2	1	1	4	4	4	4	1	1	2	1	2	1	1	2	0	0	0	0	0	0	0	0
ID22			OD	588		17.7;9.47@4E	10.5	-1		0 Blue	2	1	1	1	4	4	4	4	0	0	1	0	0	0	1	0	0	0	1	0	0	0	0	0	0
ID22	26	1	OS	575		17.8;0.17@184	10	-1		0 Blue	1	2	1	2	4	4	4	4	0	0	1	1	0	1	0	0	0	0	0	0	0	0	0	0
ID23			OD	579		15.7;9.17@175E	9	-3.25		0 Blue	1	1	1	1	4	4	4	4	0	0	1	1	2	1	3	3	0	0	0	0	0	0	0	0	0
ID23	28		OS	571		15.7;8.67@77E	9	-2.75		0 Blue	1	1	1	1	4	4	4	4	0	0	1	1	0	3	3	3	0	0	0	0	0	0	0	0	0
ID24			OD	527		13.7;9.17@88E	10	-0.75		0 Brown	1	1	1	1	4	4	4	4	2	2	3	2	2	1	1	1	0	0	0	0	0	0	0	0	0
ID24	21	0	OS	542		15.7;9.17@19E	10	-1.25		0 Brown	1	1	1	1	4	4	4	4	2	3	3	2	2	1	1	1	0	0	0	0	0	0	0	0	0
ID26			OD	572		13.8;09.17@38E	9	-0.5		0 Blue	2	1	1	2	3	4	4	4	0	1	1	0	0	0	1	0	0	0	0	0	0	0	0	0	0
ID26	28		OS	562		13.7;9.17@94E	9	-0.5		0 Blue																								
ID27			OD	556		13.8;8.17@38E	11	-0.5		0 Blue	1	1	1	1	4	4	4	4	0	0	0	0	1	2	2	2	0	0	0	0	1	0	0	0
ID27	24	1	OS	555		13.8;9.17@79E	11	-0.5		0 Blue	1	1	1	1	4	4	4	4	0	0	1	0	1	1	2	1	0	0	0	0	0	0	0	1
ID28			OD	574		19	8			0 Blue	1	1	1	1	4	4	4	4	0	0	2	1	0	0	0	0	0	0	0	0	0	0	0	0
ID28	30	0	OS	504		18	8.5			0 Blue	1	1	1	2	4	4	4	4	0	0	2	0	0	0	1	0	0	0	0	0	0	0	0	0
ID30			OD	532		15.6;8.63@18	10	2.75		0 Blue	2	1	1	1	4	4	4	4	0	0	1	0	0	0	1	0	0	0	0	0	0	0	0	0	0
ID30	24	2	OS	534		15.6;2.63@54E	10.5	3		0 Blue	1	1	1	1	4	4	4	4	0	0	1	0	0	0	0	0	0	0	0	0	0	0	0	0
ID31			OD	585		19.6;0.27@36E	9	1		0 Blue	1	1	1	1	4	4	4	4	0	0	1	0	0	1	1	0	0	0	0	0	1	0	0	0
ID31	22		OS	565		22.7;9.17@1E	9	0.75		0 Blue	1	1	1	1	4	4	4	4	0	1	1	0	1	2	2	2	0	0	0	0	0	0	0	0
ID32			OD	539		13.7;8.17@73E	8.5	-1.25		0 Blue	2	2	3	3	4	4	3	4	0	0	1	0	0	0	1	0	0	0	0	0	0	0	0	0
ID32			OS	541		14.7;8.17@19E	8.5	-1		0 Blue	0	2	2	0	4	4	4	4	0	1	1	0	0	1	1	0	0	0	0	0	0	0	0	0
ID33			OD	589		15.7;9.17@79E	9	-0.25		0 Blue	1	1	1	1	4	4	4	4	0	0	1	0	0	0	0	0	0	0	0	0	0	0	0	0
ID33	21		OS	581		14.7;9.17@7E	9.5	-0.25		0 Blue	1	1	1	1	4	4	4	4	0	1	1	0	0	0	0	0	0	0	0	0	0	0	0	0
ID35			OD	527		12.8;3.50@180	8	-7.5		0 Brown	1	1	1	1	4	4	4	4	1	1	3	1	3	3	0	0	0	0	0	0	0	0	0	0
ID36	21	0	OS	536		12.8;4.00@166	8	-10		0 Brown	1	1	1	1	4	4	4	4	1	1	3	1	3	3	0	0	0	0	0	0	0	0	0	0

Annex 3: Recruitment flyer

Har du lyst å bli med i en studie med et nytt kamera som tar bilder av øyets kammervinkel?

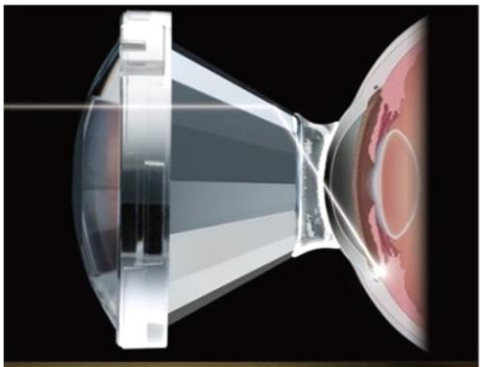

Hvilken studie er dette?
Mastergradsprosjektet "Distribution of gonioscopic findings in young adults assessed by means of 360-degree goniophotography with the Nidek GS-1 Gonioscope" har som mål å undersøke funn i kammervinkelen hos 18-35 åringer med et nytt unikt kamera. Prosjektet er et samarbeidsprosjekt mellom USN og Rodenstock Norge.

Hva innebærer det?
Deltagelse i studien medfører at kammervinkelen i øynene dine fotograferes med et Nidek GS-1 goniokamera. Fotograferingen er smertefri og synet påvirkes ikke. Undersøkelsen foregår på USN campus Krona. Totalt tar undersøkelsen maksimalt 40 minutter på et tidspunkt som passer deg.

Hvorfor stille opp?
Kunnskap om funn i øyets kammervinkel hos en ellers frisk, ung befolkning er begrenset. Du vil være med å bidra til dette. Du kan også selv lære mer om kammervinkelen og du får selvsagt tilsendt bildet om ønskelig.

Er du nysgjerrig og vil vite mer om prosjektet eller om deltakelse, ta kontakt med **Kristian Brekstad**
kristian.brekstad@gmail.com tlf 95 24 21 38